

Review

# Fracture Behaviour of Aluminium Alloys under Coastal Environmental Conditions: A Review

Ibrahim Alqahtani \*, Andrew Starr and Muhammad Khan 

Centre for Life-Cycle Engineering and Management, School of Aerospace, Transport and Manufacturing, Cranfield University, College Road, Cranfield MK43 0AL, UK

\* Correspondence: i.alqahtani@cranfield.ac.uk

**Abstract:** Aluminium alloys have been integral to numerous engineering applications due to their favourable strength, weight, and corrosion resistance combination. However, the performance of these alloys in coastal environments is a critical concern, as the interplay between fracture toughness and fatigue crack growth rate under such conditions remains relatively unexplored. This comprehensive review addresses this research gap by analysing the intricate relationship between fatigue crack propagation, fracture toughness, and challenging coastal environmental conditions. In view of the increasing utilisation of aluminium alloys in coastal infrastructure and maritime industries, understanding their behaviour under the joint influences of cyclic loading and corrosive coastal atmospheres is imperative. The primary objective of this review is to synthesise the existing knowledge on the subject, identify research gaps, and propose directions for future investigations. The methodology involves an in-depth examination of peer-reviewed literature and experimental studies. The mechanisms driving fatigue crack initiation and propagation in aluminium alloys exposed to saltwater, humidity, and temperature variations are elucidated. Additionally, this review critically evaluates the impact of coastal conditions on fracture toughness, shedding light on the vulnerability of aluminium alloys to sudden fractures in such environments. The variability of fatigue crack growth rates and fracture toughness values across different aluminium alloy compositions and environmental exposures was discussed. Corrosion–fatigue interactions emerge as a key contributor to accelerated crack propagation, underscoring the need for comprehensive mitigation strategies. This review paper highlights the pressing need to understand the behaviour of aluminium alloys under coastal conditions comprehensively. By revealing the existing research gaps and presenting an integrated overview of the intricate mechanisms at play, this study aims to guide further research and engineering efforts towards enhancing the durability and safety of aluminium alloy components in coastal environments.



**Citation:** Alqahtani, I.; Starr, A.; Khan, M. Fracture Behaviour of Aluminium Alloys under Coastal Environmental Conditions: A Review. *Metals* **2024**, *14*, 336. <https://doi.org/10.3390/met14030336>

Academic Editors: Umberto Prisco, Tomasz Tański, Francesca Borgioli and Denis Benasciutti

Received: 8 February 2024

Revised: 26 February 2024

Accepted: 13 March 2024

Published: 15 March 2024



**Copyright:** © 2024 by the authors. Licensee MDPI, Basel, Switzerland. This article is an open access article distributed under the terms and conditions of the Creative Commons Attribution (CC BY) license (<https://creativecommons.org/licenses/by/4.0/>).

**Keywords:** fatigue crack growth; fracture toughness; aluminium alloys; coastal environments; temperature; humidity; corrosion

## 1. Introduction

In the engineering world, the initiation and propagation of cracks in the material components of aircraft structures are difficult challenges that demand attention. If failure remains undetected in its early stages, it can result in severe consequences, ultimately leading to catastrophic damage. The catastrophic damage to the structures will be more expensive to replace. For this reason, researchers have performed extensive research to find solutions and minimise crack growth.

Engineering materials, particularly metals, are prone to developing cracks and fractures during service. Numerous application structures, including those in automotive, aircraft, and power plants, operate under diverse loading conditions [1]. These structures, particularly those made of aluminium alloys, become increasingly susceptible to fatigue and failure under the combined influence of mechanical loads [2]. Aluminium alloys are

essential in engineering because they provide a balance of strength and light weight [3–6]. Further technological advances enhanced the aluminium alloy, allowing it to be used in the aerospace industry [7]. Aluminium alloys in aircraft structures are advantageous due to their corrosion resistance, durability, and low maintenance requirements [8]. These properties collectively contribute to structures' effectiveness and sustainability in challenging corrosive conditions.

In corrosive conditions, environmental factors such as temperature and humidity impact the fatigue growth and fracture behaviour of aluminium alloys [9]. Researchers can evaluate a material's ability to withstand cracks or other defects caused by the corrosive environment or other loading conditions by analysing its fracture toughness [10]. High fracture toughness values indicate that a material is less likely to experience sudden failures [11], making it more reliable for corrosive environments. The combined influence of the temperature and humidity creates unique challenges to the material properties. These conditions can accelerate material degradation and cause structural failures [12]. Therefore, addressing the interaction of materials and structures with such harsh conditions is essential.

This literature review presents the significant efforts of the past and reviews the experimental and modelling challenges on fracture and fatigue crack growth under a corrosive environment. Focusing on qualitative descriptions of fracture behaviour in aluminium alloys is crucial due to their widespread use across industries. Qualitative analysis is instrumental in ensuring the safety and reliability of structures by identifying potential failure modes such as fatigue cracks and stress corrosion cracking. By studying fracture surfaces, researchers can detect manufacturing defects and impurities influencing the material's fracture behaviour. This analysis aids in understanding corrosion-related fracture behaviour, facilitating the development of alloys with enhanced corrosion resistance for applications in corrosive environments. Moreover, qualitative analysis allows tailoring alloys for specific purposes by comprehending the impact of different compositions and heat treatments on fracture behaviour. Overall, this approach contributes to a deeper understanding of the relationships between microstructure, alloy composition, and fracture properties, providing a foundation for further advancements in the field of aluminium alloys.

The literature review provides an overview of the research complexities in the coastal environment. This review organises the previous research under four significant approaches: the fundamentals of fracture and fatigue crack growth behaviour, coastal environmental conditions and their effects, fracture mechanisms in coastal environments, and modelling and predictive methods. The conclusion highlights the need for comprehensive efforts to address existing gaps in the current research field.

## 2. Fundamentals of Fracture and Fatigue Crack Growth Behaviour

In the context of materials engineering and science application, a crack refers to a discontinuity in the structure of a material, which can be initiated by various factors such as manufacturing defects, stress, fatigue, or corrosion. Crack formation in aluminium is influenced by various manufacturing-related factors that must be carefully considered to ensure the structural integrity of the material. Inclusions, impurities, and porosity arising from incomplete refinement or casting processes can act as stress concentration points, initiating cracks. Welding issues, such as incomplete fusion or a lack of penetration, can create weak zones susceptible to cracking. Heat treatment effects, including improper processes or quenching, may lead to variations in hardness and microstructural defects. Alloy composition and exposure to hydrogen during manufacturing can also affect aluminium's susceptibility to cracking [13]. The appearance of a crack is influenced by the material's microstructure, loading conditions, and environmental factors. Within engineering applications, the frequent use of fracture toughness and fatigue crack growth values attends to characterizing and evaluating the material's performance and integrity [14]. Fracture toughness represents a material's resistance to crack propagation under stress, ensuring its ability to withstand flaws and defects. On the other hand, the fatigue crack growth rate

examines how cracks initiate and propagate over time under cyclic loading conditions, offering essential insights into the fatigue behaviour of materials [15]. Researchers and engineers rely on these fundamental principles to ensure the durability and safety of structures in different applications.

Crack initiation is a complex process integral to understanding the failure of materials and structures, particularly in the realm of fatigue and fracture mechanics. The initiation of cracks often occurs under cyclic loading conditions, where repeated or fluctuating stress is applied to a material. Microscopic defects, impurities, or inclusions within the material act as stress concentration points, creating localised areas of increased stress. These stress raisers promote the nucleation of cracks, marking the initiation phase. Moreover, material flaws such as inhomogeneities, microstructural defects, or manufacturing imperfections can serve as natural sites for crack initiation. Environmental factors, such as corrosion or exposure to aggressive chemicals, further accelerate this process by degrading material properties and promoting crack formation. Overloading, exceeding a material's capacity, can induce localized plastic deformation, creating conditions conducive to crack initiation, particularly in brittle materials.

The stress intensity factor ( $K$ ) plays a pivotal role in fracture mechanics, offering a quantitative measure of stress concentration near the tip of a crack. It is expressed by the Equation (1):

$$K = \sigma\sqrt{\pi a} \quad (1)$$

where  $K$  is the stress intensity factor,  $\sigma$  is the applied stress, and  $a$  is the crack length. This factor is essential for evaluating the severity of stress near the crack tip and understanding crack growth behaviour. As the stress intensity factor increases, it approaches a critical value known as fracture toughness ( $K_{Ic}$ ). This critical point signifies the threshold beyond which crack propagation becomes unstable, leading to catastrophic failure. The stress intensity factor aids in predicting under what conditions cracks will propagate, guiding engineers in designing structures to avoid failure due to crack growth. In essence, it provides a critical parameter for assessing the susceptibility of materials to fracture, ensuring the reliability and safety of engineering components subjected to various loading conditions [16].

There will be yielding ( $\sigma_{ys}$ ) and a plastic zone due to the postulated infinite elastic stresses at the fracture tip. Irwin determined the size of the plastic zone ( $r_y$ ) [17]; Equation (2):

$$r_y = \frac{1}{2\pi} \left( \frac{K_{Ic}}{\sigma_{ys}} \right)^2 \quad (2)$$

A more precise estimate of the size of the plastic zone ( $r_p$ ) considers the redistribution of stresses when the zone begins to yield; Equation (3):

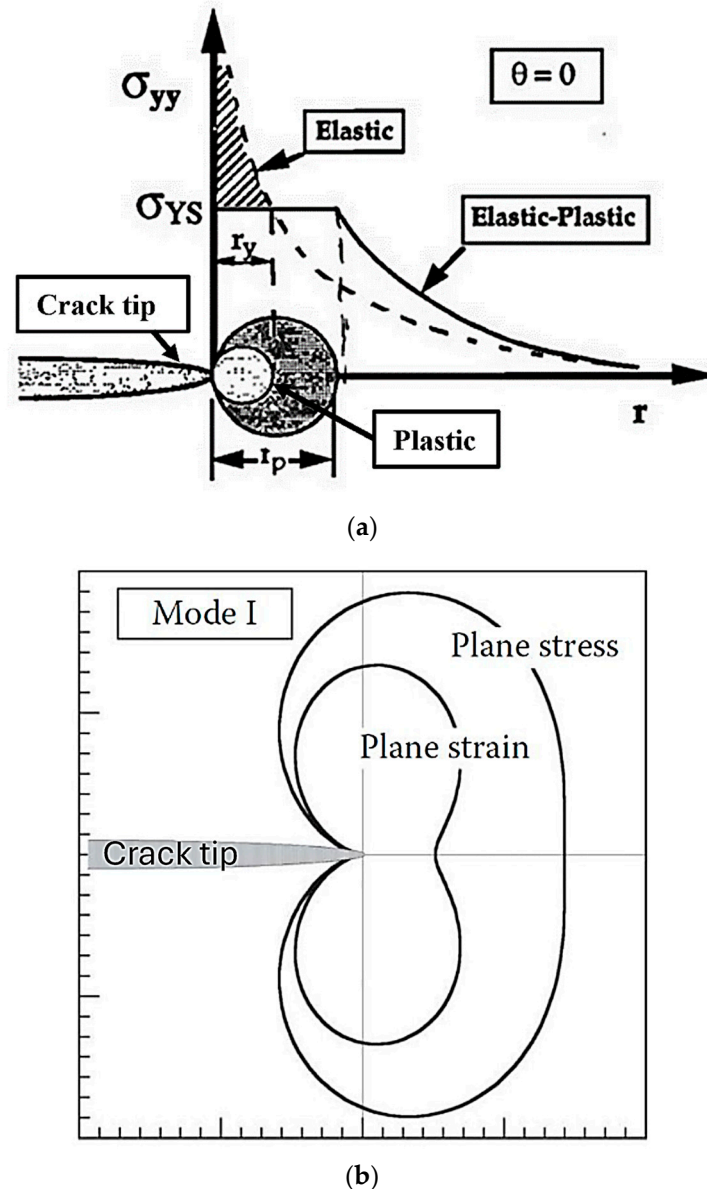
$$r_p = 2r_y = \frac{1}{\pi} \left( \frac{K_{Ic}}{\sigma_{ys}} \right)^2 \quad (3)$$

Figure 1a illustrates this redistribution effect,  $r$  indicates the radial distance from the crack tip, and  $\sigma_{yy}$  represents the stress in the radial direction. The plastic zone's geometry under plane stress and plane strain conditions is illustrated in Figure 1b.

### 2.1. Fracture Toughness

Fracture toughness measures a material's capacity to resist the crack growth [18]. The quantification and establishment of standardised fracture toughness are achieved through the application of fracture mechanic theories such as linear elastic fracture mechanics (LEFM) and elastic-plastic fracture mechanics (EPFM) [19]. These theories find widespread use in the evaluation of structural integrity, residual strength analysis, fitness-for-service assessments, and the design of damage-tolerant structures [11]. Consequently, the assessment and testing of fracture toughness have become crucial for advancing the practical engineering applications of the fracture mechanics approach [16]. After recognising this

importance, the American Society for Testing and Materials (ASTM) stipulated standardised terminology and procedures for fracture toughness testing and assessment. These guidelines are outlined in fatigue and fracture testing E1820 [20] and linear-elastic plane strain fracture toughness of metallic materials E399 [21].



**Figure 1.** (a): Crack tip plasticity. (b): Crack tip plastic zone shapes and the von Mises yield criterion.

Figure 2 illustrates the three distinct modes of loading, Mode I, Mode II, and Mode III, that can be applied to a crack. Mode I involves forces pulling the crack surfaces apart, often encountered in tensile scenarios. Mode II features sliding forces along the crack plane, essential for plane shear or sliding stress analysis. Mode III involves forces that make one side of the crack move out-of-plane shear, leading to tearing. Many standard geometries of specimens in materials testing, such as compact tension (CT), disk-shaped compact specimen (DCT), arc-shape (AS) specimen, and single-edge notch bend (SENB) specimens, are designed for opening loading Mode I during testing, as shown in Figure 3A [16]. These specimens are specifically engineered to apply controlled tensile forces to study various material properties, including fracture toughness and fatigue crack growth [16]. Doddamani et al. [15,22–24] studied how various geometric parameters affect fracture toughness in Mode I. Also, they utilised different specimen types, including CT, SENB, and

circumferential notched tensile (CNT) specimens, and their findings indicate that all these specimen types produced consistent results.

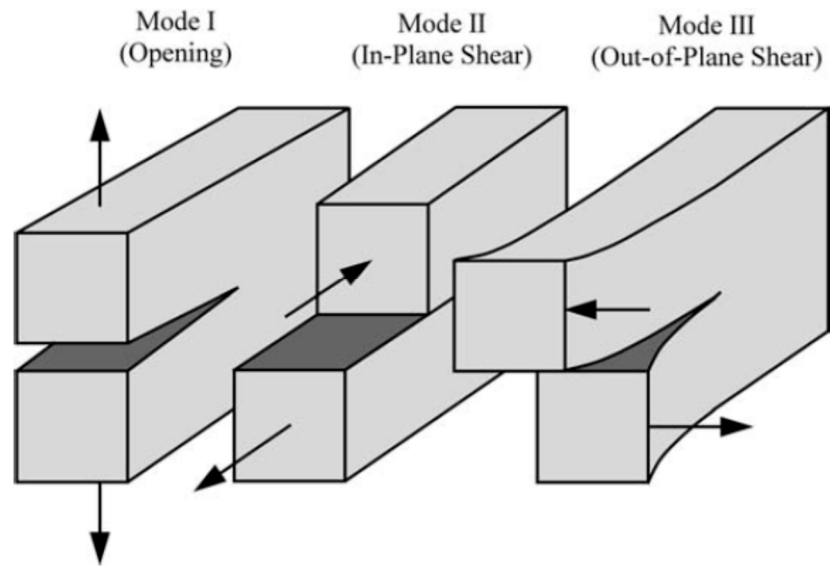


Figure 2. Three loading modes imposed on a crack. Adapted from ref. [16].

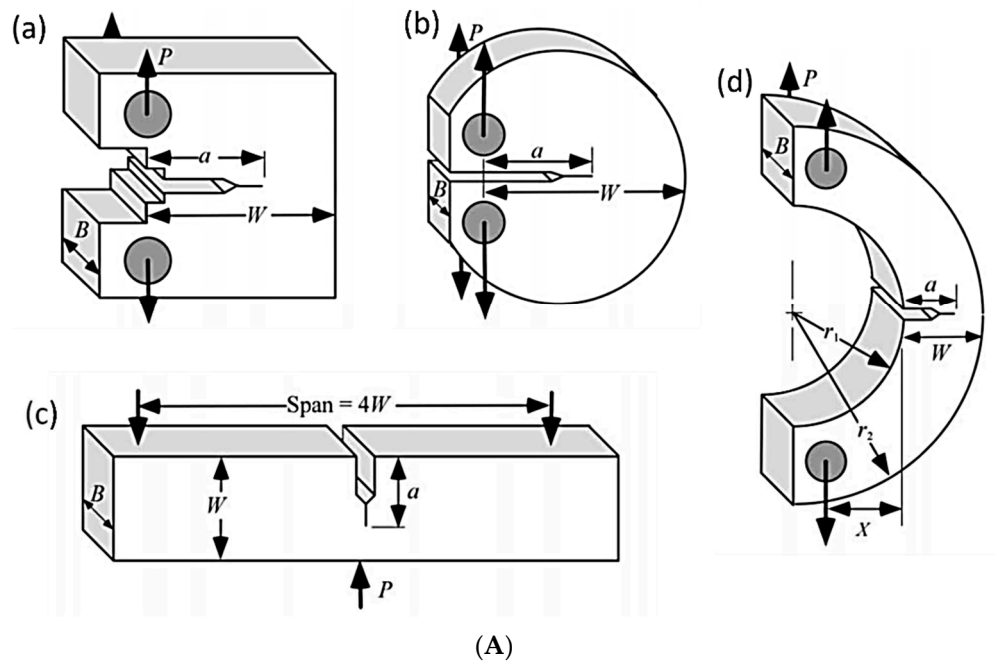
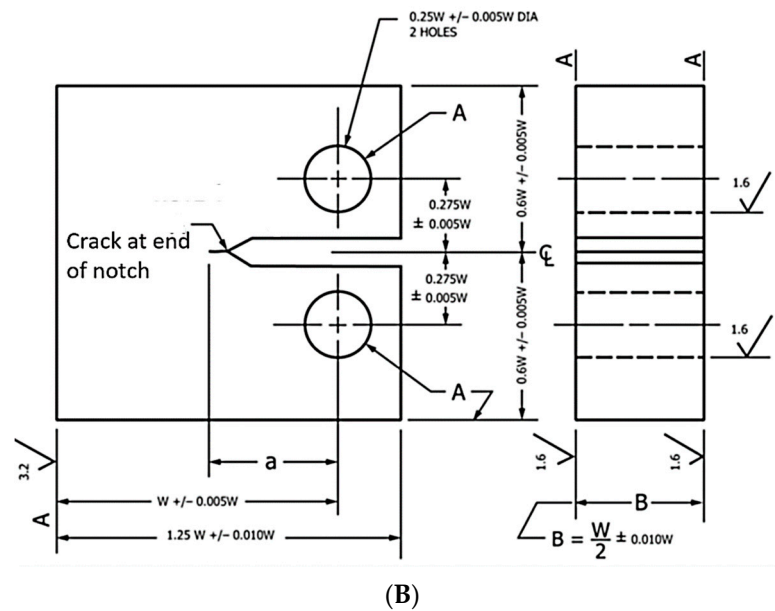


Figure 3. Cont.



**Figure 3.** (A): Standardised test specimens: (a) CT, (b) DCT, (c) SENB, and (d) AS specimen adapted from ref. [16]. (B): Geometry of CT specimen. Adapted from ref. [21].

Researchers [8,12,25–28] generally prefer CT specimens for fracture toughness testing due to their standardised nature, widespread acceptance, and the assurance of consistent and comparable outcomes. CT specimens are well-suited for Mode I crack propagation, which is common in engineering applications, and they create near-plane strain conditions, simplifying crack growth analysis. Figure 3B illustrates the geometry of the CT specimen employed in fracture toughness testing, as per ASTM E399 standard.

The fracture toughness testing machine records the load and the crack mouth opening displacement data with three distinct curves, as shown in Figure 4. The three different types are Type I, II, and III, as classified by ASTM E399 [21].

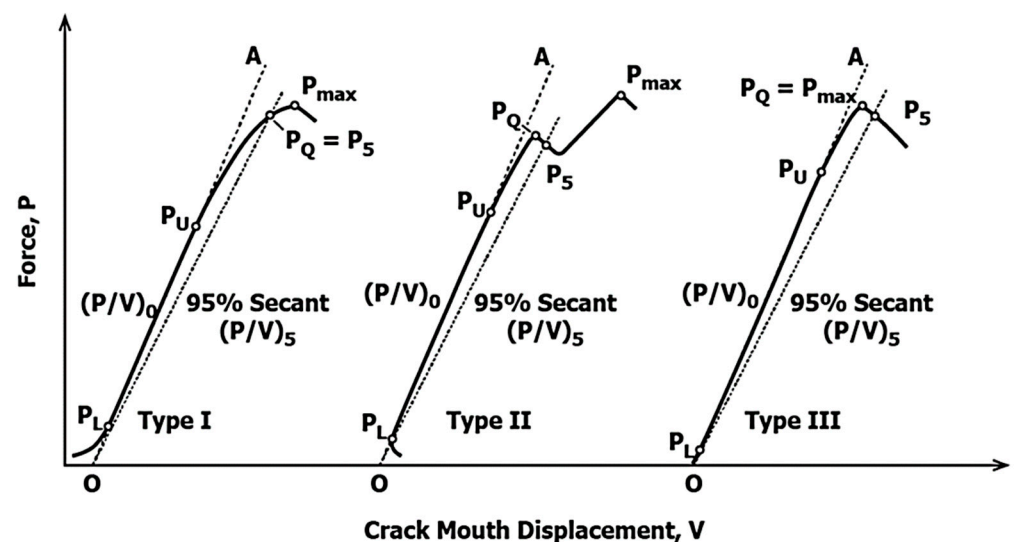


**Figure 4.** Load vs. CMOD curves. Adapted from ref. [21].

The ASTM E399 standard introduced a method to define the conditional stress intensity factor ( $K_Q$ ), which depends on the value of conditional load  $P_Q$  and maximum load  $P_{max}$ . Conditional load value  $P_Q$  is determined by the secant line ( $OP_5$ ) with a slope  $(P/V)_5$  equal to 0.95 times the slope of the tangent  $OA$  between  $(PL)$  and  $(PU)$ , denoted as  $(P/V)_0$ . In

practical terms, when determining the secant line  $OP_5$ , the pivotal point for adjusting the slope rotation should align with the intersection of the line OA and the displacement axis. The force  $P_Q$  is subsequently defined as follows: if the maximum force occurs after  $P_5$  (Types I and II), then  $P_5$  is designated as  $P_Q$ . In cases where a preceding maximum force before  $P_5$  surpasses it (Type III), this preceding maximum force is acknowledged as  $P_Q$  [21].

Determining the critical load  $P_Q$  at a 95% secant offset contributes to achieving the valid plane strain fracture toughness value,  $K_{Ic}$ , which depends on calculating the  $P_{max}/P_Q$  ratio. This ratio serves as validation criteria, ensuring the fracture toughness measurement complies with the specified testing standards and maintains reliability [29]. The fracture toughness of metallic material was determined using the Equation (4) [21].

$$K_Q = \frac{P_Q}{\sqrt{BB_N}\sqrt{W}} f\left(\frac{a}{W}\right) \quad (4)$$

where, for CT Specimens,

$$f\left(\frac{a}{W}\right) = \frac{\left(2 + \frac{a}{W}\right)}{\left(1 - \frac{a}{W}\right)^{\frac{3}{2}}} \left[ 0.886 + 4.64\left(\frac{a}{W}\right) - 13.32\left(\frac{a}{W}\right)^2 + 14.72\left(\frac{a}{W}\right)^3 - 5.6\left(\frac{a}{W}\right)^4 \right]$$

The condition for the plane strain fracture toughness is given in Equations (5) and (6) below [30]:

$$B \geq 2.5 \left(\frac{K_Q}{\sigma_y}\right)^2 \quad \text{and} \quad a \geq 2.5 \left(\frac{K_Q}{\sigma_y}\right)^2 \quad (5)$$

$$W \geq 5.0 \left(\frac{K_Q}{\sigma_y}\right)^2 \quad (6)$$

where  $B_N$  is the thickness of the specimen at the notch,  $B$  is the thickness of the specimen,  $a$  is the crack length,  $W$  is the specimen width,  $P_{max}$  is the load-carrying capacity,  $\sigma_y$  is the yield strength of the material.

## 2.2. Fatigue Crack Growth Rate (FCGR)

FCGR is a measure used to quantify the rate at which a crack in a material grows over time under cyclic loading conditions. Consequently, ASTM E647 is a standard test method that provides guidelines for measuring the FCGR in metallic materials. CT specimens are frequently employed in FCGR testing due to their standardised geometry, which ensures precise and replicable testing conditions. Also, it requires the least amount of test material to evaluate crack growth behaviour. Their suitability for investigating crack propagation is attributed to a simplified analysis of crack growth rate [31].

Figure 5 illustrates a comprehensive schematic fatigue crack growth curve, explaining distinct regimes in the progression of cracks under cyclic loading conditions. In the initial regime, short/small fatigue cracks initiate at discontinuities, showcasing exponential growth. This transitions into a second regime with non-inspectable slow fatigue crack growth (FCG), marking a critical juncture. Short/small cracks evolve into 0.25–0.5 mm long/large cracks in aluminium alloys, representing in-service inspectable FCG. Subsequently, increased fatigue loads expedite crack growth, ultimately leading to component failure [32].

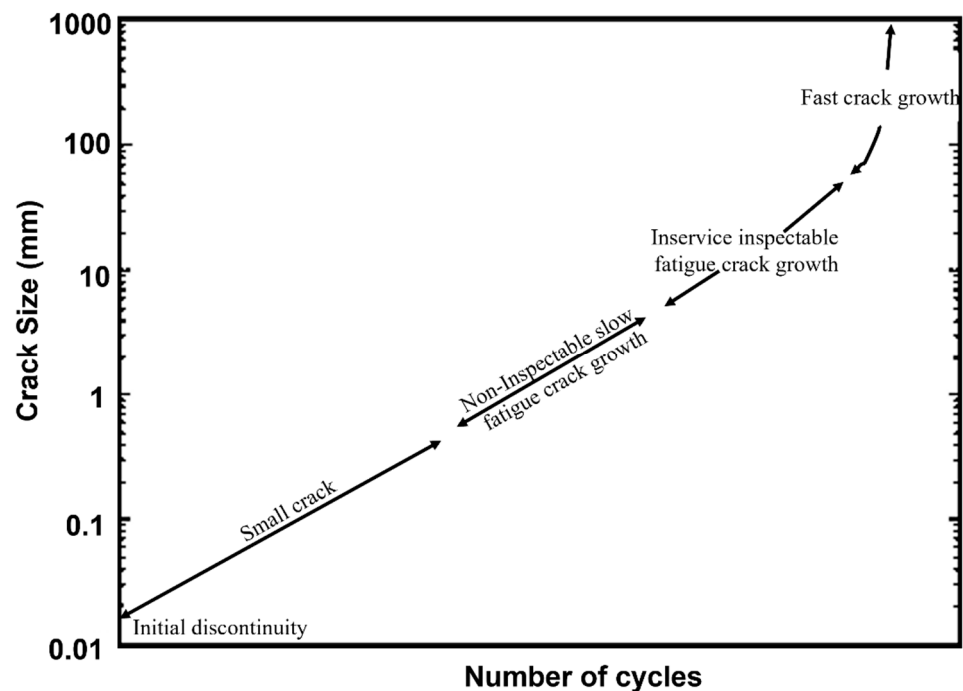


**Figure 5.** Schematic fatigue crack growth curve showing different regimes of crack growth. Adapted from ref. [32].

All the following authors used the CT specimens and established the standard procedure for fracture and fatigue testing of aluminium alloys and their composites. Lee [33] focused on assessing the fatigue crack growth performance of aluminium metal matrix composites (MMCs). R. Yuan et al. [34] performed tests to evaluate fracture toughness and cyclic fatigue properties of aluminium alloy and its composites. Abdul Budan et al. [35] studied the fatigue and mechanical characteristics of Al6061 aluminium alloy and composites. Y. Uematsu et al. [36] conducted fatigue tests at elevated temperatures, employing smooth specimens of aluminium alloy and its composites with diverse particle sizes while keeping a consistent weight percentage of silicon carbide (SiC) particles. D. P. Myriounis et al. [37] investigated the fatigue and fracture toughness characteristics of aluminium reinforced with SiC particles. J. Huang et al. [38] studied the impact of microstructural variability on the very high-cycle fatigue behaviour of discontinuously reinforced aluminium metal matrix composites (MMCs). Sharma et al. [39] investigated the fatigue characteristics of the aluminium alloy, and their experimental results showcased improvements in the fatigue and fracture properties of the material. Bikash Joadder et al. [40] performed experimental and finite element analyses to predict failure cycles. Shahani et al. [41] employed CT specimens to estimate methods for fatigue life prediction. Furthermore, numerous other researchers [42,43] conducted similar experiments on CT specimens to predict fatigue life.

A crack employed at the end of the notch, shown in Figure 3, can be introduced using a servo-hydraulic testing machine [8]. The prepared CT specimen is securely mounted in the grips of the testing machine. Crack initiation is then started by applying controlled loading conditions, such as load ratio, frequency, and strain rate [44]. Even though employing digital image correlation (DIC) and/or high-speed camera [45] techniques, monitoring crack propagation carefully throughout the fatigue testing process is challenging.

Fatigue in materials exposed to repetitive cyclic loading can be described as a developing process involving three stages: regime I, which is crack initiation; regime II, which is stable crack propagation as per Paris law; and regime III, unstable crack propagation or fracture failure, shown in Figure 6 [46]. The Paris law is an empirical equation used to model materials' fatigue crack growth rate. Using a power-law equation plotted in logarithmic coordinates, Paris' law (Equation (7)) establishes a connection between the

stress intensity factor range ( $\Delta K$ ) and the crack growth rate ( $da/dN$ ). The alterations made to Paris' law for determining crack growth rates proved highly effective in enhancing the accuracy of fatigue life predictions in engineering design [47].

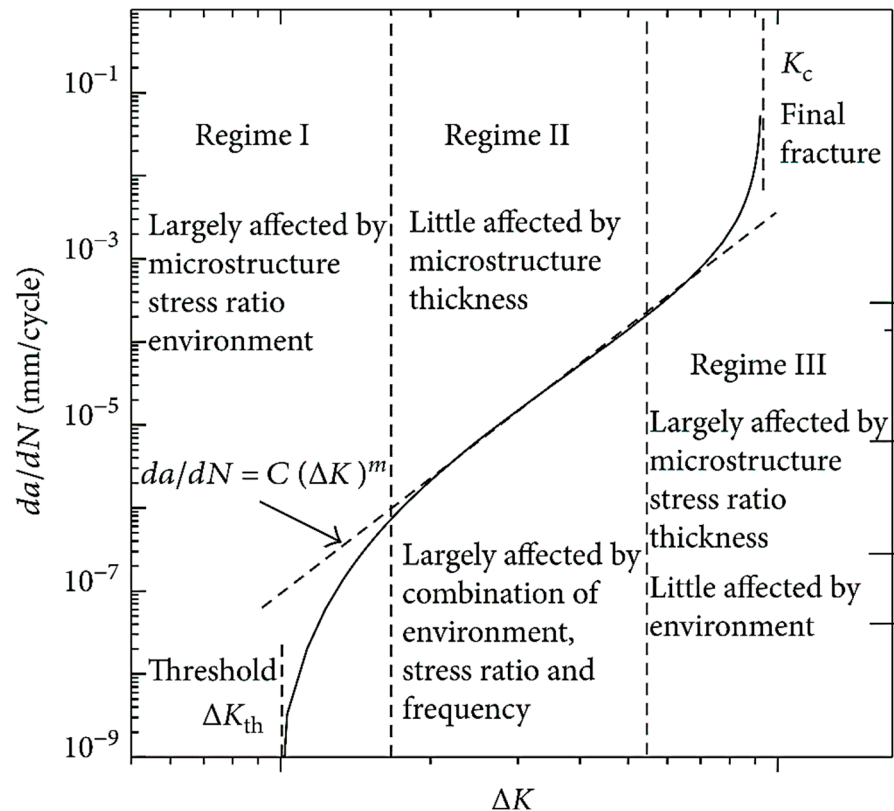


**Figure 6.** The stress intensity factor curve for metallic materials typically exhibits three distinct regimes when it comes to fatigue crack growth rate. Reprinted from ref. [47].

### 2.3. Environmental Fracture

Figure 6 depicts the curve correlating the stress intensity factor with the fatigue crack growth rate. Moreover, the figure visually represents the regimes of fatigue crack growth rate that are notably impacted by environmental factors. Environmental factors such as temperature, humidity, and exposure to corrosive agents are commonly encountered in coastal regions [48]. In a corrosive medium, regime I still begins with small crack initiation, but it happens faster due to corrosion weakening the material at potential stress points [49]. This can lead to the formation of tiny corrosion-induced cracks, often detectable only under a microscope. During regime II, when small cracks expand, the corrosive agents attack the crack tips, promoting rapid material degradation and creating a favourable environment for crack growth [50]. Cracks can spread more quickly and deeply compared to non-corrosive conditions, posing a significant threat to material integrity [51]. In regime III, the corrosive medium intensifies rapid crack advancement, potentially resulting in unstable crack propagation. Cyclic loading, combined with corrosion-induced weakening, leads to a sudden failure and severe loss of structural strength [52]. The cross-sectional area of the material reduces further due to corrosion, thus increasing the risk of unexpected failure.

Several deterministic FCGR functions have been proposed and extensively used in the determination of fatigue crack development rate under corrosive conditions [53]. These functions include the Trantina–Johnson Equation (8), Walker Equation (9), and Forman Equation (10). Although adjustments were made to account for varying stress ratios, the Paris model is only capable of explaining linear or stable fracture growth rates at a given

stress ratio. Nonetheless, Equation (7) is still utilised to describe the behaviour of corrosion fatigue crack development (FCG) [53].

$$\frac{da}{dN} = C(\Delta K)^m \quad (7)$$

Trantina–Johnson Model:

$$\frac{da}{dN} = C(\Delta K - \Delta K_{th})^m \quad (8)$$

Walker Model:

$$\frac{da}{dN} = C(\Delta K)^{m_1} (1 - R)^{m_2} \quad (9)$$

Forman model:

$$\frac{da}{dN} = C \frac{(\Delta K)^m}{(1 - R)K_c - \Delta K} \quad (10)$$

where  $\frac{da}{dN}$  is the crack growth per stress cycle,  $\Delta K$  is the stress intensity factor (SIF) range;  $R$  is the stress ratio;  $K_c$  is the fracture toughness depending on the thickness of the specimen;  $a$  is the crack length or size;  $C$  is the material-specific Paris constant;  $m$ ,  $m_1$ ,  $m_2$  are the material constant; and  $\Delta K_{th}$  is the threshold stress intensity factor.

One of the primary environmental factors affecting fatigue crack growth is corrosion. Materials can be specifically engineered to resist corrosion by selecting corrosion-resistant alloys or incorporating corrosion inhibitors. Applying protective coatings is a common strategy to shield materials from environmental factors. These coatings act as barriers, preventing direct contact between the material and corrosive agents or environmental moisture [54]. Various coating materials, such as polymers, ceramics, or corrosion-resistant paints, can be tailored to provide an additional layer of defence against environmental degradation, thus slowing down fatigue crack initiation and growth [55].

The composition and microstructure of materials play a vital role in their response to environmental factors. By carefully selecting alloying elements and controlling the microstructural features, engineers can enhance the material's resistance to fatigue crack growth. Advances in material science and technology offer opportunities to develop innovative materials with superior fatigue resistance. Nanotechnology, for instance, allows for the creation of nanostructured materials with unique mechanical and environmental resistance properties [56]. Designing materials for enhanced durability involves considering the entire lifecycle of the material, from manufacturing to usage and eventual disposal. Sustainable materials and manufacturing processes that minimize environmental impact contribute to a more holistic approach to material design.

#### 2.4. Threshold Stress Intensity Factor

The threshold stress intensity factor ( $\Delta K_{th}$ ) indicates the minimum stress intensity required to initiate stable crack growth in a material [57]. The crack growth testing data was utilised to determine  $\Delta K_{th}$  values. The linear Paris curve was studied in the evaluation process to extrapolate the values corresponding to extremely low crack growth rates, such as  $10^{-10}$  m/cycle or  $10^{-6}$  mm/cycle [58]. This extrapolation aids in estimating the threshold stress-intensity range, shown in Figure 6.

Perez N [59] studied the linear Paris growth–rate curve to estimate the threshold stress-intensity range, making the critical limiting variable the threshold  $\Delta K_{th}$  value. Equation (11) states that small-crack fatigue thresholds can be calculated from the Paris law constants  $C$  and  $m$  [58,59].

$$\Delta K_{th,smallcrack} = \left( \frac{10^{-6}}{C} \right)^{\frac{1}{m}} \quad (11)$$

Corrosion-induced small cracks in materials often have a lower  $\Delta K_{th}$  than large cracks. Environmental factors influence this phenomenon, emphasising the importance of assessing

the threshold stress intensity range when evaluating the structural integrity of materials exposed to coastal conditions.

Table 1 provides a comparative overview of the fatigue strength and fracture toughness of various aluminium alloys, presenting key mechanical properties essential for assessing their performance in structural applications.

**Table 1.** Fatigue strength and fracture toughness of different aluminium alloys [45].

Al Alloy	Elastic Modulus (GPa)	Yield Strength (MPa)	Fatigue Strength (MPa)	Fracture Toughness (MPa·√m)	Reference
AA6061	68–74	193–290	207	18.21	[60]
AA6082	67.1	276	-	19–25	[60]
AA7075	71	482	-	27.5	[61]
AA7050	70–80	455	240	27.5	[62]
AA2024	72–75.7	345–381	138	18.5	[63]
AA5083	70–73.6	269–297	-	28.3	[64]
AA8090	77	370	100	28	[65]

### 3. Coastal Environmental Conditions and Their Effects

The coastal region experiences intense, dry summers and high humidity [66]. These climatic particulars underscore the challenges of coastal region environmental conditions, particularly for materials, infrastructure, and equipment exposed to these harsh coastal environments. The corrosive nature of the coastal environment, characterised by exposure to saltwater, high humidity, and temperature, challenges the durability and integrity of various engineering materials [67]. You Tang et al. [68] conducted a study investigating how the coastal environment and concentration of salt ions affect the materials and structures. These conditions have a saltwater potential to advance material corrosion due to the corrosive nature of salt ions. Figure 7 illustrates the unique challenges and environmental factors that structures in coastal areas are exposed to, which can substantially impact their integrity and durability.

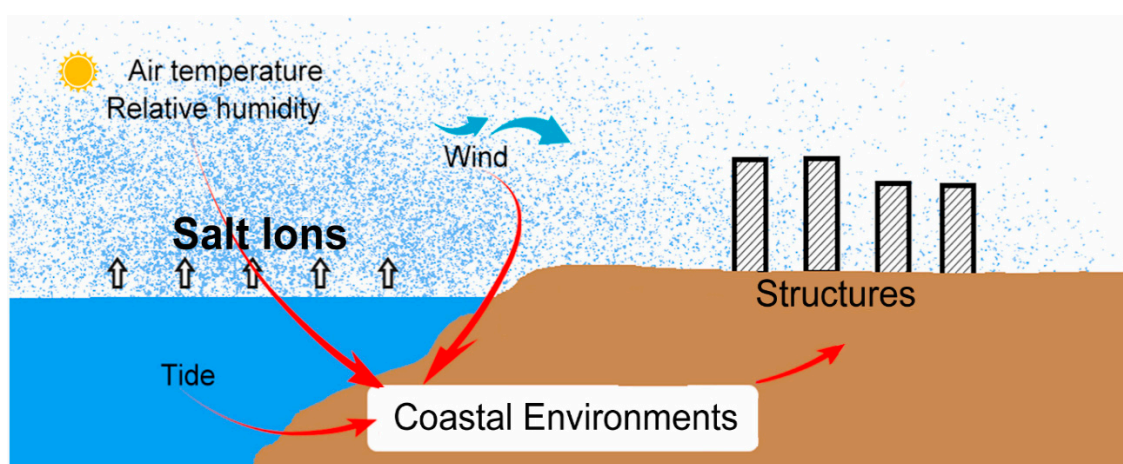


**Figure 7.** Typical coastal environment conditions on nearby structures.

Additionally, coastal areas are marked by higher humidity levels, mainly due to their proximity to vast bodies of water. This higher humidity can induce moisture absorption by materials, resulting in possible corrosion. It was observed that temperature variations are common in coastal areas, leading to thermal damage that influences fatigue perfor-

mance and long-term durability [69]. Furthermore, the occurrence of marine vaporisers in coastal regions, comprised of airborne seawater droplets and particles, amplifies corrosion processes by depositing corrosive salts on structural surfaces.

### 3.1. Simulation of Coastal Conditions

Simulation of coastal conditions involves creating controlled laboratory environments that mimic the environmental factors found in coastal areas. This simulation is critical for studying how materials, such as aluminium alloys, react to the unique challenges of coastal environments.

#### 3.1.1. Corrosion Simulation

Ramesh et al. [12] studied the fracture toughness of the aluminium alloy under a corrosive environment using CT specimens. In this work, the corrosion simulation of aluminium alloys was accomplished by immersing prepared CT specimens in a 3.5% sodium chloride (NaCl) solution for a specified number of days. Cavalcante et al. [70] and Y Zheng et al. [71] chose a 3.5% NaCl solution for the immersion, as it closely replicates the salinity of seawater. Similarly, Zakaria [72] also mentioned in his research that the specimens are subjected to immersion in the 3.5% NaCl solution for a specified number of days, with the duration based on the research objectives and the desired level of corrosion simulation.

Specimens can be immersed in actual seawater from a coastal area to simulate natural conditions [73]. Alternatively, synthetic seawater solutions can be prepared to mimic the composition of natural seawater. B J Little et al. [74] mentioned the composition of synthetic seawater solutions, which often include salts like NaCl, MgCl<sub>2</sub>, CaCl<sub>2</sub>, and other ions found in seawater. Researchers can control each component's concentration for precise corrosion studies in this approach.

Over time, the corrosion process on the surface of the aluminium alloy specimens is initiated and accelerated by the NaCl solution, replicating the corrosion observed in coastal regions due to salt ions in the atmosphere and water. After the specified immersion period, the specimens are carefully removed from the NaCl solution, cleaned, and thoroughly examined [75].

#### 3.1.2. Environmental Chamber

Sarah et al. [76] used the environmental chamber to simulate the induced crack on the specimens. An environmental chamber replicates the typical conditions available in coastal regions [77]. Sahand et al. [78] and Faridah et al. [79] mentioned the environmental chamber, also called the climate chamber, that precisely controlled temperature and humidity levels. Coastal environments are characterised by notable temperature fluctuations, ranging from elevated daytime temperatures to cooler nighttime conditions [80]. Temperature cycling can be implemented within the environmental chamber to replicate these daytime variations accurately. Furthermore, maintaining high humidity levels is necessary for accurately simulating coastal conditions. The climate chamber offers the capability to finely control humidity levels, creating a humid atmosphere similar to that experienced in coastal regions. This controlled setup is essential for scientific investigations aiming to replicate and study the effects of temperature variations and high humidity available in coastal environments on material behaviour.

The specimens are positioned within the environmental chamber for a predetermined duration [76]. Since utilising the environmental chamber represents a novel technique, standardising its procedural application becomes essential. This standardisation ensures consistency and repeatability in the experimental process, enabling reliable and comparable results. Once this exposure period is completed, the samples are retrieved from the environmental chamber. Subsequently, they were immediately taken to the testing machine through the desiccator [81] and fixed in the machine for mechanical testing. The desiccator maintains the specified temperature and humidity conditions until the specimens are ready to be taken to the mechanical testing machine [82]. This step is essential to prevent

changes in the specimens' condition and properties between the exposure phase and the subsequent testing. This instant transition ensures that the specimens are assessed quickly after exposure to the simulated coastal conditions, enabling the accurate evaluation of their material properties and performance.

### 3.2. Effect of Corrosive Solution

Aluminium alloys are susceptible to corrosion when they are exposed to a NaCl solution. Corrosion can lead to pits and cracks on the material's surface. These defects can act as stress concentrators and reduce the material's fracture toughness [12]. The cyclic loading and exposure to a corrosive environment, such as a NaCl solution, could result in corrosion fatigue. This phenomenon occurs when the cyclic stresses applied to the material work in conjunction with the corrosive environment to accelerate crack growth [83]. Ramesh et al. [12] mentioned in their research that aluminium typically develops a protective oxide layer on its surface in atmospheric conditions. However, the presence of corrosion pits can significantly disrupt the uniformity of this oxide layer [84]. This effect is particularly pronounced with a longer duration, resulting in a defective oxide layer.

Notably, the intermetallic compounds commonly found in Al6000 alloys, the  $Mg_2Si$  phase, and AlFeSi particles [85] are noteworthy. AlFeSi particles can cause localised corrosion in the surrounding matrix because they function as cathodic phases [86]. Conversely, the  $Mg_2Si$  phase is less noble than the adjacent Al matrix [87], creating a potential difference promoting localised corrosion at the interface. Additionally, corroded samples often accumulate corrosive ions on their surfaces, such as  $Cl^-$ , which inevitably interact with the oxide film, compromising its corrosion resistance.

Figure 8 provides a schematic representation of the localised corrosion process observed in the Al6061 alloy. In the initial stages of corrosion, chloride ions ( $Cl^-$ ) penetrate the matrix through imperfections originating from either the AlFeSi or  $Mg_2Si$  particles. This penetration leads to the dissolution of the oxide film that typically protects the metal surfaces, consequently initiating pitting corrosion, as mentioned by Can Peng et al. [88]. An oxide layer, in the context of corrosion, refers to a protective film that forms on the surface of a metal exposed to environmental conditions. This layer consists of metal oxides and can act as a barrier, preventing further corrosion by isolating the metal from the surrounding environment.

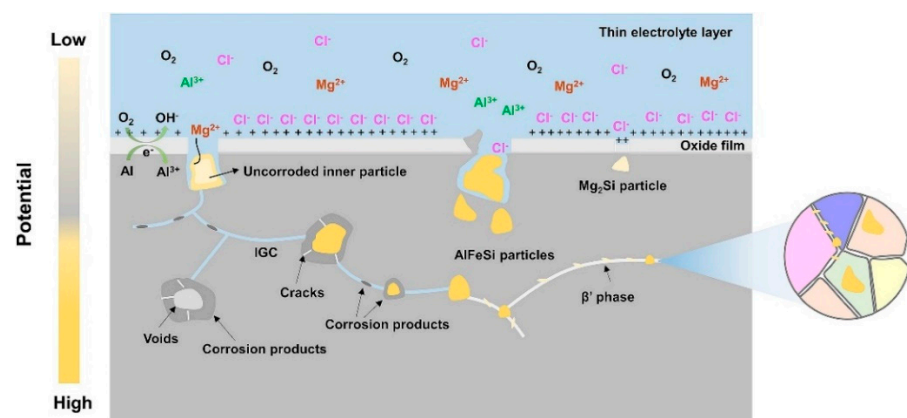


**Figure 8.** Diagrammatic representation of the Al6061 alloy's corrosion process in a marine environment. Reprinted with permission from ref. [88] Copyright 2022 Elsevier.

Pits are small, localised cavities that form on the surface of a material due to exposure to a NaCl solution [89]. They are typically deeper than they are wide and can penetrate the material, compromising its integrity. This leads to the formation of cracks and corrosion products, which decreases corrosion resistance, as shown in Figure 9. Corrosion products are compounds or substances that result from the chemical reactions between a metal and

its environment during the corrosion process. Peng et al. [88] mentioned that corrosion products, such as metal oxides, hydroxides, and salts, often contribute to the visible changes in the appearance of a corroded surface.

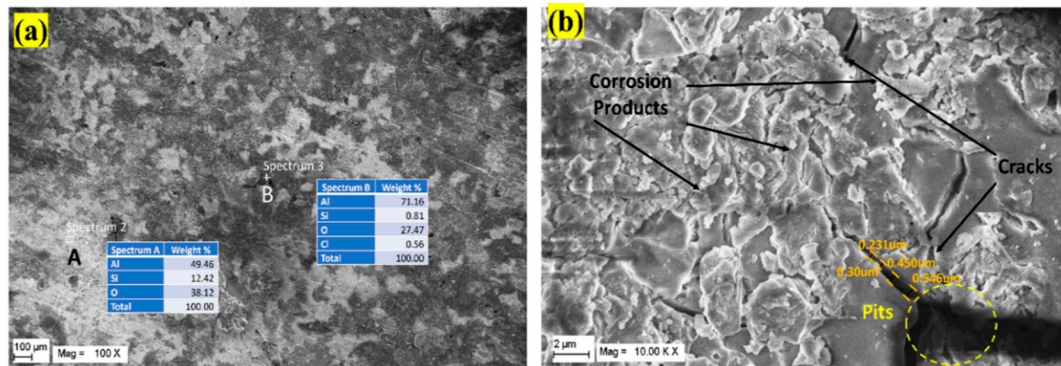


**Figure 9.** Corroded samples showing (a) oxide layer, (b) corrosion products, cracks, and pits. Reprinted with permission from ref. [12] Copyright 2023 Elsevier.

### 3.3. Effect of Temperature

The effect of temperature in coastal regions on the fracture toughness and FCGR of aluminium alloys is influenced by saltwater, humidity, and exposure to marine atmospheres. Coastal temperatures generally exhibit moderate effects due to the influence of large bodies of water. The combination of temperature variations and humidity can contribute to the degradation of material properties [90].

According to the researchers [91–93], environmental variables were responsible for the failures of aircraft components made of aluminium alloys while in service. The corrosive environment significantly influenced the operation of the aircraft components in coastal areas. Temperatures exceeding 70 °C may result from the heat generated by aircraft equipment during its operation, potentially impacting component performance [94].

Otieno et al. [95] and Zheng et al. [71] worked on aluminium alloys and a chloride medium in marine exposure environments. From the outcomes, it can be reported that temperature can increase the salinity of seawater, making it more aggressive [71]. Structures can be impacted by the evaporation of hazardous airborne chemicals such as chlorides [95]. On the other hand, faster and deeper chloride penetration causes the material to develop microscopic cracks and corrosion pits. The rate of chloride penetration and its depth into the material is influenced by factors like temperature and the diffusion coefficient.

Vargel et al. [96] collectively identified pitting corrosion in an aluminium alloy subjected to corrosion within 20 to 80 °C. However, aluminium is susceptible to pitting corrosion at room temperature and in a higher pH range (8.1 for seawater) [94]. In marine environments, the oxide layers, FeO, Al<sub>2</sub>O<sub>3</sub>, CuO, and ZnO, were formed at 30–60 °C [90]. The tendency for pitting corrosion gradually reduces at temperatures of 70 °C and up to 150 °C when an aluminium oxide layer forms [96].

Cao et al. [90] conducted a thorough investigation to enhance the comprehension of the corrosion characteristics exhibited by the 2A02 aluminium alloy. They subjected samples of the 2A02 alloy to 200 h of corrosion exposure at 30 °C, 60 °C, and 80 °C. As the temperature increased from 30 °C to 60 °C and further to 80 °C, it became evident that the number of pits decreased accordingly, as shown in Figure 10a.

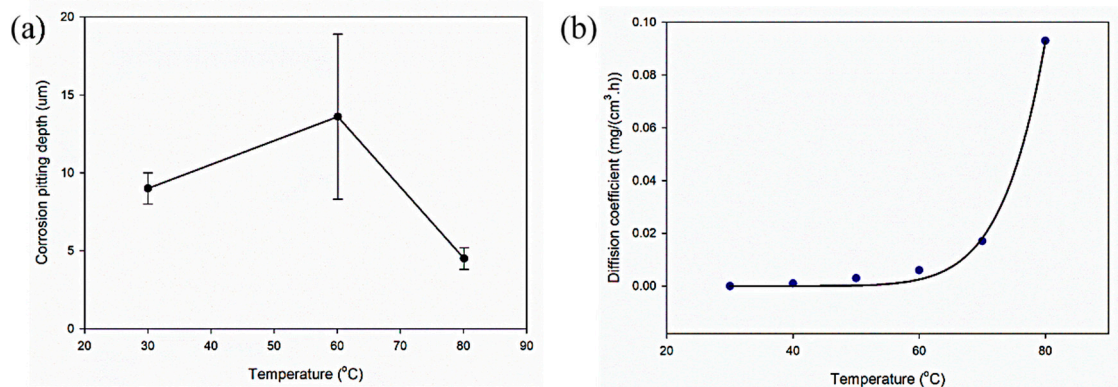


**Figure 10.** Effect of temperature and corrosion on aluminium alloy: (a) corrosion depth and (b) diffusion coefficient relationship trend chart [90].

Figure 10b, illustrating the correlation between temperature and the diffusion coefficient, offers valuable insights into how particle or molecule diffusion varies with temperature. The diffusion coefficient is linked to the rate at which reactants or ions can migrate through the material or the oxide layer. Generally, temperature increases the diffusion coefficient [80], facilitating the more rapid diffusion of reactants, such as oxygen or water molecules [90]. This accelerated diffusion can enhance reactions at the metal–oxide interface, potentially fostering the growth of protective oxide layers.

### 3.4. Effect of Humidity

The corrosion behaviour and mechanical performance of 7085 aluminium alloy in a hot, humid marine environment are studied by Tao J et al. [97]. Humid conditions can significantly influence the material properties of aluminium alloys, often increasing the challenges posed by the marine atmosphere. Daming et al. [98] studied the corrosion resistance of aluminium alloy under high humidity conditions. High humidity levels prevalent in coastal areas enhance moisture absorption by aluminium alloys. This moisture accelerates the corrosion process when combined with the corrosive nature of salt-laden coastal air. The chloride ions in the air can penetrate the alloy's surface, initiating and accelerating corrosion, leading to surface degradation, pitting, and the formation of corrosion products, as mentioned by Ramesh et al. [12].

Sarah Dorman et al. [99] worked on corrosion fatigue under moist air atmospheric conditions in samples with surface salt deposits. The result concludes that the structure and component are often subjected to cyclic loading under moisture conditions, which can lead to fatigue failure. In humid conditions, combining moisture and salt particles can further reduce the fatigue life of aluminium alloys by promoting faster crack growth rates. This effect is particularly detrimental, as it can compromise the long-term durability of structures. Intergranular and pitting corrosion are common localised types of corrosion observed in humid coastal environments, as mentioned by Yingchang et al. [100]. These types of corrosion can develop cracks, voids, and localised material degradation, affecting the material's structural integrity. Bray et al. [101] work on moist air and state that humid conditions can alter the mechanical properties of aluminium alloys. This may include reductions in tensile strength, flexibility, and toughness. These changes can affect the load-bearing capacity and overall structural performance of components and structures.

Ahmad [102] and Bradshaw et al. [103] worked on gaseous environments and the corrosion of aluminium alloys. When the relative humidity in the gaseous environment exceeds the equilibrium relative humidity over any saturated solution on the metal's surface, atmospheric corrosion occurs. This is particularly important for aluminium alloys, highlighting that the ambient air acts as a corrosive medium, causing chemical reactions on fracture surfaces through atmospheric moisture [103].

Davidson et al. [104] studied the effect of water vapour and ambient air on fatigue crack tip mechanics in Al7075 alloy. When aluminium is subjected to cyclic loading in ambient air, its fracture growth rates rise, and its threshold stress intensities drop in comparison to vacuum circumstances. Moisture causes a fracture tip's ability to tolerate cyclic plastic strain to decrease, which leads to this phenomenon. According to Holper et al. [105], diffusion carries water vapour from the ambient air to the tip of the crack, where it initiates chemical interactions with exposed fracture surfaces to produce hydroxide, hydrated oxides, and hydrogen absorption.

Young et al. [106] and Mahdih Safyari et al. [107] worked on the hydrogen embrittlement mechanisms and mentioned that cracking in humid air is more accurately described as hydrogen-environment-assisted cracking. According to Equation (12) provided below, the reaction of water vapour at the alloy surface can result in hydrogen atoms that have the potential to be absorbed into the alloy and then recombine to generate H<sub>2</sub> gas [106]:



where X is the degree of hydration, g is gas (vapour), and s is solid.

These detailed studies regarding coastal environments help cultivate an understanding of the combined effect of various factors in corrosive conditions. The combined effects of these conditions also need to be understood by the multiple mechanisms explained in further sections.

#### 4. Fracture Mechanisms in Coastal Environments

Fracture and fatigue crack growth involve the initiation, expansion, and eventual instability of cracks within materials. In coastal conditions, factors like corrosion, temperature fluctuations, and humidity play critical roles in these processes, as mentioned by Sarah et al. [99,108]. In the fracture process, small cracks usually originate at stress concentration points or material flaws and slowly develop under cyclic loading. In the case of fatigue crack growth, Khodor et al. [109] mentioned the microscopic defects within the material, which can evolve into small cracks due to repeated cyclic stresses. González et al. [110] thought that, in humid environments, corrosive agents can speed up crack initiation. As these cracks initiate, they may gradually propagate through the material, with the rate of growth influenced by factors like material properties, stress levels, and environmental conditions.

The mechanisms associated with fracture and fatigue crack growth in metals involve various elements and occurrences essential for understanding the initiation and propagation of cracks and their interactions with the corrosive environment. The following are the fracture mechanisms identified to occur in corrosive environmental conditions.

##### 4.1. Oxide Layer

Studying the effect of the oxide layer in crack initiation and propagation is essential, particularly in coastal regions where the presence of salt and moisture is common. Understanding the beginning and spread of cracks, especially in corrosion conditions like those seen in coastal locations, depends on an oxide layer on the surface of materials like aluminium alloys [111].

Oxide layers frequently and naturally occur on metals exposed to air conditions [112]. As seen in Figure 11, these layers serve as protective barriers that prevent the metal surface from touching corrosive substances like moisture and salts available in corrosive areas. This protection is vital because it helps delay or prevent crack initiation [113]. The oxide layer can enhance the material's corrosion resistance by reducing the rate at which the underlying metal corrodes [114]. This is essential in coastal regions where the corrosive nature of salt ions, NaCl, in the atmosphere can accelerate material degradation. By impeding corrosion, the oxide layer plays a key role in preserving the material's integrity and structural strength [115]. However, the oxide layer is not always uniformly perfect [116] and can have defects or imperfections, which can become potential sites for crack initiation [117].

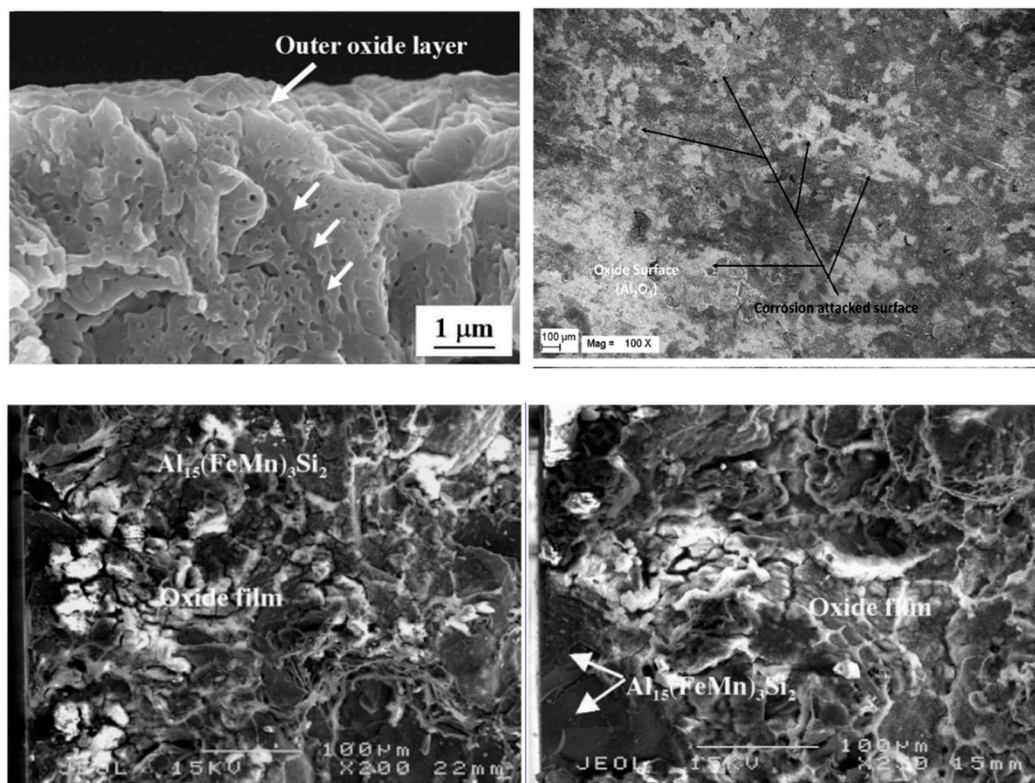


**Figure 11.** Oxide layers formed on aluminium alloys. Reprinted with permission from ref. [12] Copyright 2023 Elsevier, [118], reprinted with permission from ref. [119] Copyright 2013 Taylor & Francis.

The presence of oxide layers on metal surfaces, particularly in coastal regions, is crucial for preventing corrosive substances like moisture and salts from initiating cracks. While these layers enhance corrosion resistance, defects in the oxide layer can become potential sites for crack initiation, highlighting the importance of studying their effects on material integrity.

#### 4.2. Crack Closure

At the fracture tip, the phenomenon of crack closure acts as a mechanism to lessen the crack's driving force [120]. Yamada et al. [121] highlighted, in their research, that crack closure plays a significant role in governing crack growth behaviour. Pokorny et al. [120] mentioned the residual plastic deformations, the roughness on the crack surfaces, and debris formation along these surfaces partially drive the crack closure phenomenon.

As illustrated in Figure 12, several elements, such as an oxide layer, phase particles, and plastic deformation in front of the crack tip, impact crack closure. This can temporarily reduce the effective stress intensity factor ( $K_{eff}$ ), which drives crack propagation, helping to extend the life of aluminium structures exposed to corrosive conditions. Cracks can initiate and propagate due to the corrosive attack on the material's surface in the presence of corrosion, which is common in coastal environments.

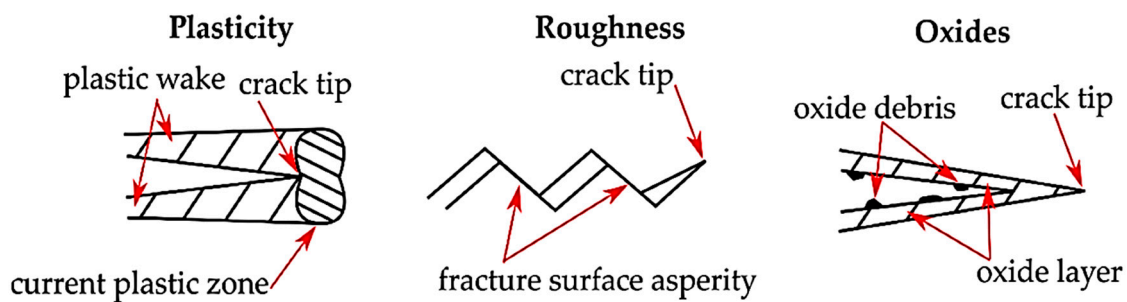


Figure 12. Crack closure mechanisms. Reprinted from ref. [120].

Moreover, coastal regions often experience temperature variations and high humidity levels [95]. The wide temperature range in coastal regions results in the expansion and contraction of materials, including aluminium structures. This thermal expansion and contraction can cause thermal fatigue [80], which leads to the narrowing of existing cracks, a form of crack closure [122]. The elevated humidity levels in coastal areas can introduce moisture to the cracks in aluminium structures. This moisture can initiate corrosion or oxidation processes, potentially causing the formation of corrosion products on the crack surfaces [12]. The formation of corrosion products causes the surface's roughness, partially closing the crack, and contributes to the crack closure mechanism [123].

Crack closure at the fracture tip, influenced by factors like an oxide layer and plastic deformations, temporarily reduces the effective stress intensity factor, extending the life of aluminium structures in corrosive coastal conditions. Temperature variations and high humidity in coastal regions lead to thermal fatigue and moisture-induced corrosion, contributing to crack closure mechanisms and influencing crack propagation in aluminium structures.

#### 4.3. Phase Particles

The formation of phase particles in aluminium alloys exposed to coastal environmental conditions, including corrosion, temperatures up to 50 °C, and humidity levels reaching 95%, is a multifaceted process influenced by various interacting factors. Alloy composition is pivotal, as elements like magnesium, silicon, and manganese can precipitate out of the aluminium matrix under specific conditions, as mentioned by Culliton et al. [124].

Figure 13a depicts the formation of intermetallic phase particles in a corrosion medium. It also illustrates different types of phase particles formed on various aluminium alloys, as seen in Figure 13b,c. Dessi et al. [125] and Shrivastava et al. [126] studied the chloride-induced corrosion on aluminium alloys. They concluded that corrosion, driven by chloride ions from saltwater, can alter the microstructure and contribute to phase particle formation.

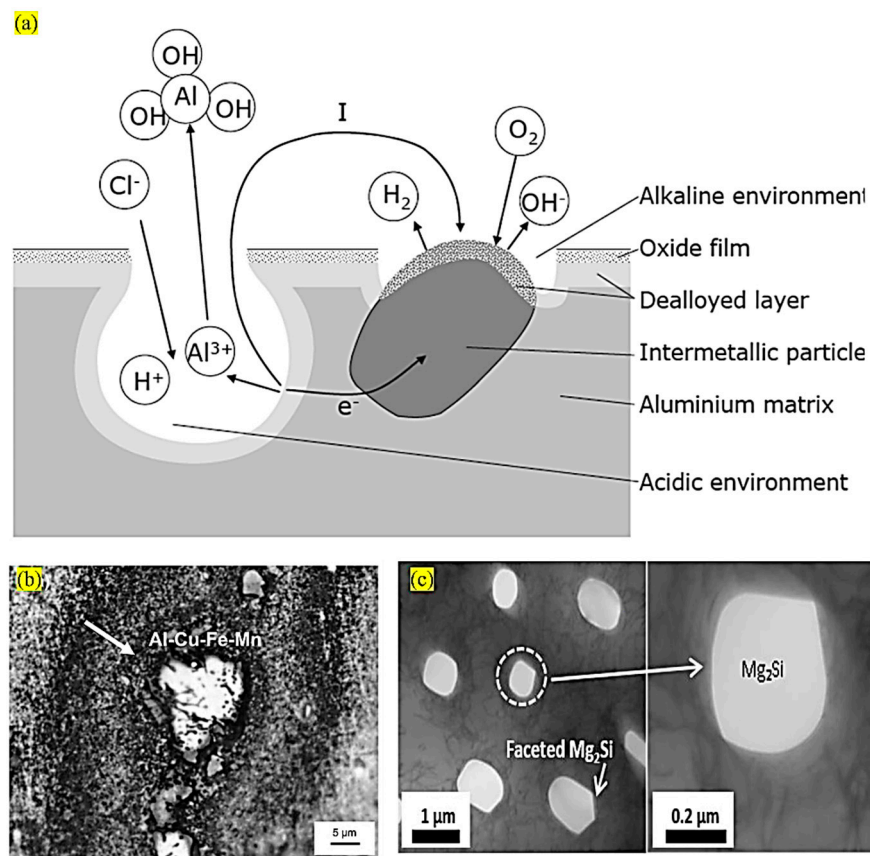


**Figure 13.** (a) Formation of intermetallic particles in corrosion medium. Reprinted from ref. [127]; (b,c) different phase particles formed on other aluminium alloys. Reprinted from ref. [128,129].

Blau P J [130] studied the mobility of alloying elements at elevated temperatures and concluded that temperature enhances alloying elements' mobility, promoting their interaction and subsequent particle formation. Gain et al. [131] and Arrabal et al. [132] worked on the Sn–Ag–Cu and Mg/Al alloys, respectively, in high-humidity environments, and they concluded that high humidity levels accelerate corrosion, further influencing the material's microstructure. Cavalcante et al. [70] studied different aeronautic aluminium alloys in air and saline environments, emphasising the critical consideration of exposure duration. The cumulative effects of corrosion and humidity gradually lead to microstructural changes, including the development of phase particles. Thus, particles can form through various precipitation mechanisms depending on alloy composition, environmental variables, and other factors.

In coastal environments, alloy composition, chloride-induced corrosion, and high humidity contribute to complex processes leading to the formation of phase particles in aluminium alloys. Elevated temperatures enhance alloying elements' mobility, influencing particle formation and emphasizing the cumulative effects of corrosion and humidity over time.

#### 4.4. Striations Spaces

Fatigue striations refer to fine, repetitive patterns or lines observed on the fracture surface of a material placed to fatigue loading [133]. Monitoring and analysing fatigue striations are essential in understanding the mechanisms and behaviour of materials subjected to cyclic loading conditions, particularly in fatigue failure [134]. It was observed that a striation mechanism of failure in materials becomes prominent within the power law region or Paris law regime [135]. These striations indicate a characteristic pattern of crack growth within this regime. They occur as the crack tip repeatedly advances and changes

during each loading cycle. The spacing between fatigue striations is equivalent to the crack propagation rate in one cycle, particularly during stage II, stable fatigue crack growth [136]. However, in some instances, the distance between fatigue striations is significantly wider than the rate at which the fatigue crack propagates in a single cycle. This suggests that the striations develop over multiple cycles of cyclic damage accumulation. It is important to note that environmental factors can also influence the formation of fatigue striations [133].

The features of fatigue striations at the stable crack growth are depicted in Figure 14a–d. As seen in Figure 14d, some second-phase particles are chopped, and secondary cracks are frequently obstructed when they come into contact with the secondary-phase particles. Additionally, the dislocation will accumulate around the second-phase particles due to the dislocation reciprocating through them, which leads to stress concentration and cracks on both sides of the particles [137].

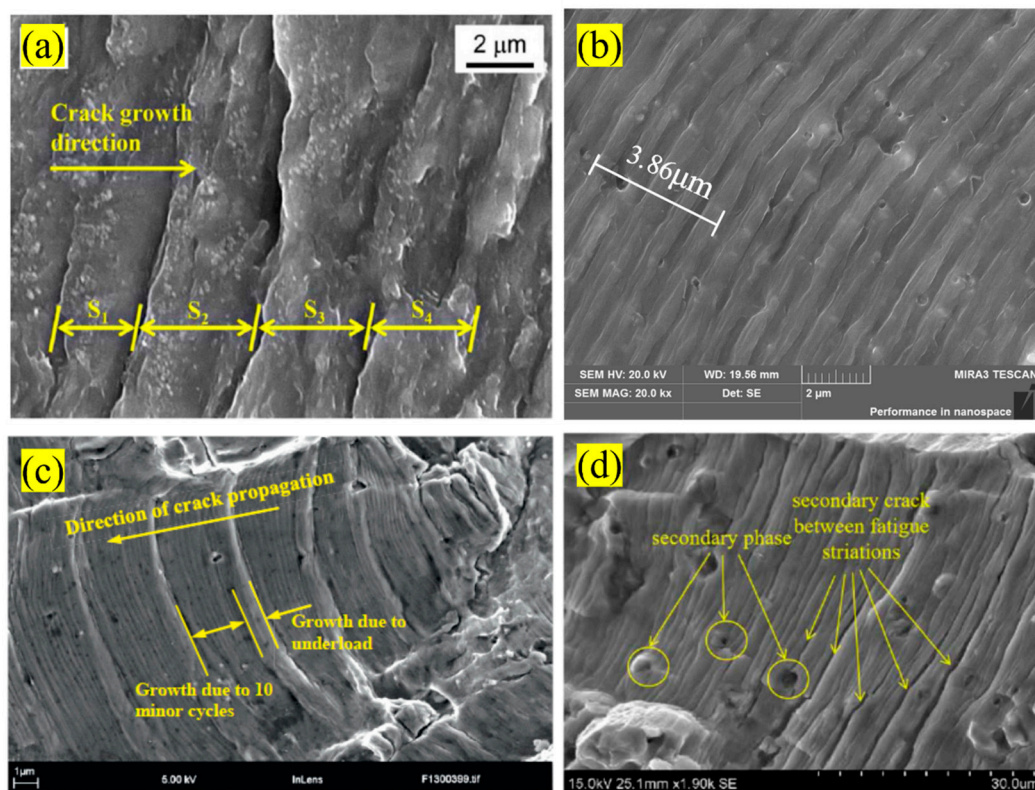


**Figure 14.** Striation spaces observed in aluminium alloys due to fatigue loading: (a) Reprinted with permission from ref. [138] Copyright 2019 Elsevier, (b) [139], (c) Reprinted from ref. [140], (d) Reprinted from ref. [137].

Due to the combined effects of fatigue and surface concentration, plastic deformation becomes confined to specific grains with favourable orientations, minimizing constraints from neighbouring grains. As the number of cycles increases, the damage progresses, giving rise to persistent slip bands (PSB) induced by shear stresses, resulting in intrusions and extrusions (stage 1). The localized damage areas give rise to microcracks, reaching sizes similar to the microstructure (e.g., Figure 15, mode II crack arrested at a grain boundary, stage 2). The early propagation of microcracks ultimately leads to the formation of macrocracks (stage 3), and subsequent engineering crack propagation leads to the final failure or fracture (stages 4 and 5). Sharma et al. [141] investigated the fatigue crack growth striation and threshold behaviour of the Al2219 alloy. Their work utilised the micrograph mapping technique, explicitly mapping the striations observed at regimes I, II, and III of the fatigue crack growth rate curve.

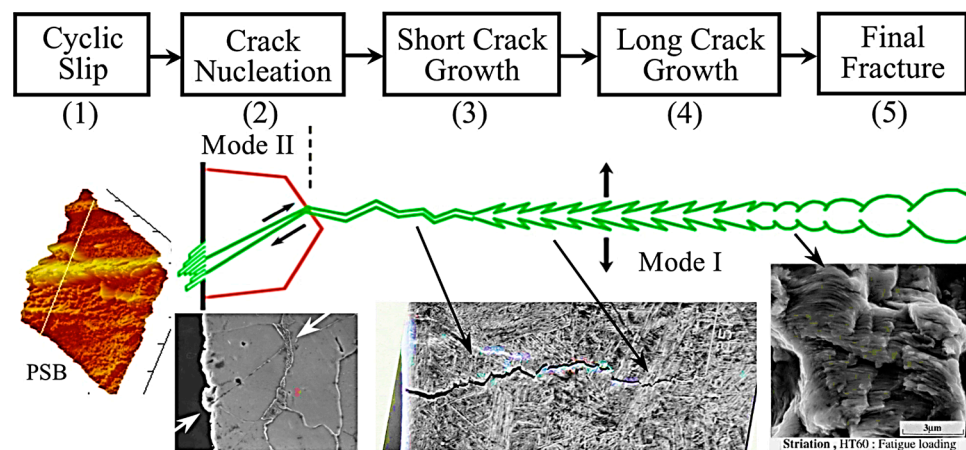


**Figure 15.** Stages of fatigue damage in metals. Reprinted from ref. [142].

In stable crack growth, the spacing between striations reflects the crack propagation rate, influenced by environmental factors. The progression from persistent slip bands to macrocracks delineates stages of fatigue damage leading to final failure, as investigated in studies on aluminium alloy.

#### 4.5. Crack Propagation Path

Capturing the crack propagation path is critical to understanding material behaviour and structural integrity. Researchers primarily rely on valuable techniques such as digital image correlation (DIC) [143] and optical microscopy for this purpose [144]. Fatigue loading repeatedly stresses the material, leading tiny cracks or imperfections on the surface to grow into small cracks over time [145]. These cracks can be challenging to detect with the naked eye. Therefore, researchers utilise digital image correlation (DIC) to monitor crack propagation and growth speed [146]. DIC can generate detailed crack maps illustrating the propagation path [147]. These maps can be analysed to understand how environmental conditions impact the direction and rate of fatigue crack growth in aluminium alloys.

Anna et al. [148] utilised a high-resolution camera positioned in the front of their experiment to continuously monitor crack propagation in the specimen. They also measured crack lengths on the surface of the CT specimens using this camera to validate data from the compliance method, as depicted in Figure 16.

The morphological characteristics of fatigue fracture of the alloy under different conditions are shown in the optical micrographs in Figure 17. Figure 17a shows the most complex expansion path with a “Z” pattern in this example. In contrast, the sample in Figure 17b exhibits a relatively straight fatigue fracture propagation path with only a slight curvature in the early stages. The fatigue fracture of the sample is shown in Figure 17c, starting gradually and developing into a curved path as it expands. Based on previous studies, complex fatigue crack growth paths indicate slower crack growth rates, supported by experimental fatigue crack growth data [136].

Understanding crack propagation paths is crucial for assessing material behaviour and structural integrity. Techniques like digital image correlation (DIC) and optical microscopy help monitor and analyze fatigue crack growth in aluminium alloys. Researchers utilize high-resolution cameras and DIC to capture and validate crack propagation data, revealing diverse patterns in fatigue fracture paths, with complex paths indicating slower crack growth rates.

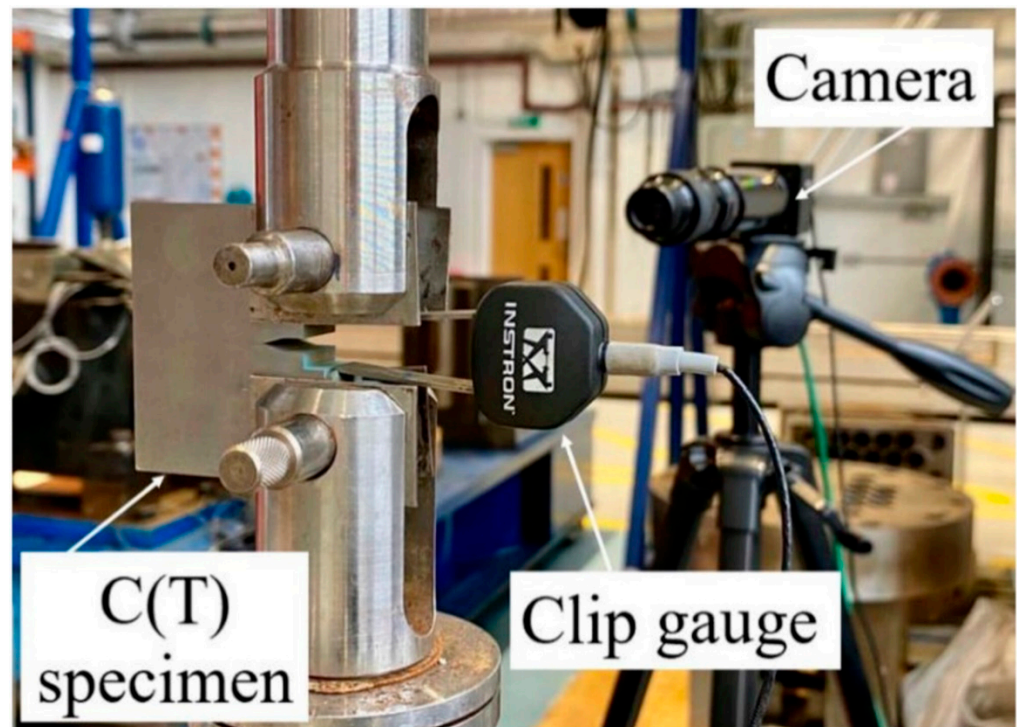


Figure 16. Experimentation setup with high-speed camera. Reprinted from ref. [148].

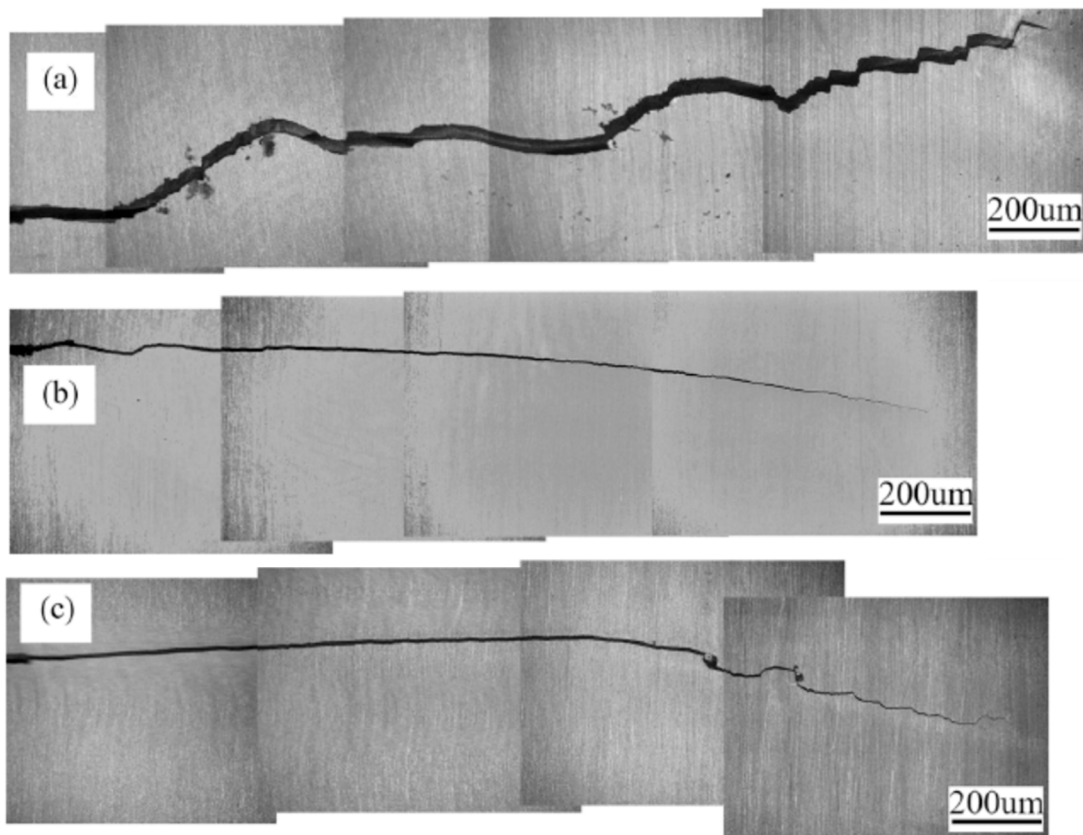


Figure 17. (a–c) Crack propagation paths showing different patterns. Reprinted with permission from ref. [136] Copyright 2022 Elsevier.

#### 4.6. Corrosion–Fatigue Interaction

Corrosion fatigue, which is viewed as a combination of two mechanical behaviours in components, is one of the most significant factors in fatigue analysis [149]. Understanding the fatigue and corrosion behaviour of these materials is crucial in specialised industries like submarines [150,151], aeroplanes [152,153], aviation engine combustion systems [154], and other applications [155,156] because of the development of new manufacturing systems in the modern world.

When a material is subjected to cyclic mechanical loading in a corrosive environment, it can degrade and experience corrosion fatigue. It is a particularly challenging and damaging form of degradation because it combines the effects of mechanical stress and chemical corrosion, leading to a more rapid deterioration of materials [157].

Corrosion fatigue often begins with microscopic defects or stress concentrators in the material [158]. In a corrosive environment, the material surface may be attacked by chemical agents, forming corrosion pits or localised corrosion [159]. When the material is subjected to cyclic mechanical loading, it introduces alternating stress on the material, which leads to the initiation and propagation of cracks from the stress concentrators or corrosion pits [160]. The cracks tend to grow incrementally during fatigue loading. The corrosive environment can accelerate crack propagation by facilitating the nucleation and growth of corrosion-assisted fatigue cracks, leading to the localised weakening of the material around the cracks [52]. Corrosion fatigue increases crack growth rate compared to purely mechanical fatigue or corrosion alone [161].

Corrosion fatigue, a significant factor in fatigue analysis, combines mechanical stress and chemical corrosion in materials subjected to cyclic loading in corrosive environments. This damaging degradation accelerates crack initiation and propagation, leading to localized material weakening and a faster deterioration rate compared to purely mechanical fatigue or corrosion alone. Understanding corrosion fatigue is crucial in specialized industries such as submarines, aeroplanes, and aviation engine combustion systems.

#### 4.7. Moisture-Assisted Crack Propagation

Moisture-assisted crack growth occurs when materials are exposed to higher humidity. This causes moisture to be absorbed and diffused into the material and promotes the formation of a thin electrolyte layer (TEL), a thin water layer on the material's surface [162]. In the presence of chloride ions, this microenvironment creates localised areas conducive to corrosion, accelerating localised corrosion processes and causing material degradation near the crack tip. Moisture promotes localised corrosion and accelerates crack growth with corrosion products (oxides, hydroxides, or chlorides) [163,164]. Moisture distribution in materials plays a crucial role in the movement of chloride ions at different depths, which was supported by Huague et al. [165].

Chloride ions are known for their corrosive nature, and their presence near the crack tip can initiate and accelerate corrosion processes. The synergy between moisture and these corrosion products significantly amplifies the localised corrosion process. As a result, the material's integrity becomes compromised and more susceptible to crack propagation [166]. This combined effect of moisture and chloride ions weakens the material's resistance to crack growth. Consequently, cracks can advance rapidly, potentially reducing the material's fatigue life [161].

Moisture-assisted crack growth in higher humidity creates a thin electrolyte layer, promoting localized corrosion and accelerating cracks with chloride ions, compromising material integrity and potentially reducing fatigue life.

#### 4.8. Hydrogen Embrittlement

The phenomenon known as “hydrogen embrittlement” occurs when hydrogen atoms seep into a material's structure, impairing its mechanical qualities and increasing its brittleness and susceptibility to failure and cracking [167]. This process can occur in various materials, including aluminium alloys. The schematic diagram of the hydrogen-enhanced

localised plasticity (HELP) mechanism is shown in Figure 18. In the HELP region, hydrogen is trapped inside the aluminium alloy through the weak areas (in the absence of an oxide layer). The plastic zone without hydrogen characterises localised deformation, crack blunting, micro-void coalescence, and deep dimples [168].

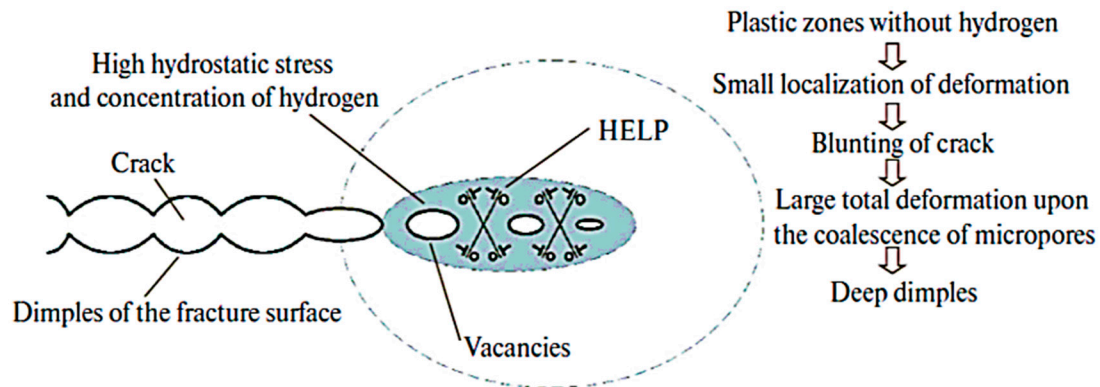


**Figure 18.** Schematic diagram of the HELP mechanism. Adapted from ref. [168].

When aluminium alloys are exposed to corrosive environments [169,170], they react with water vapour and cause hydrogen embrittlement (HE) [171], as shown in Figure 19. Hydrogen atoms can be introduced into aluminium alloys through various sources, such as exposure to moisture or corrosive environments [107]. Inside aluminium alloys, hydrogen atoms accumulate at defects, grain boundaries, dislocations, and other imperfections. These regions act as trapping sites for the accumulation of hydrogen atoms [172].

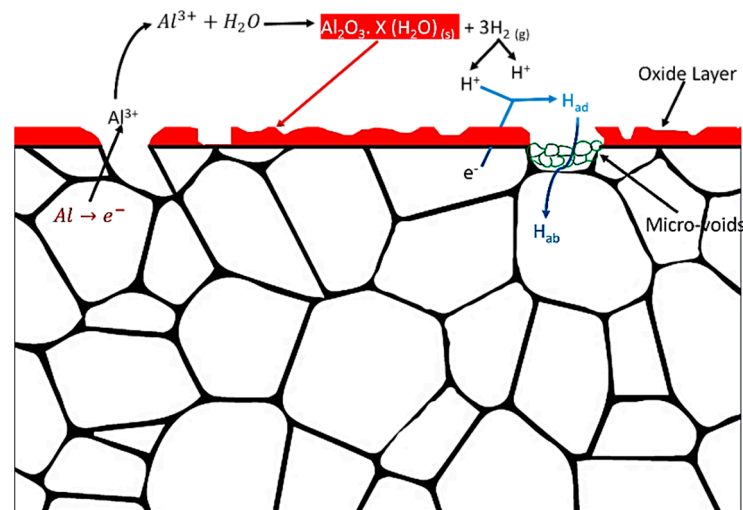


**Figure 19.** Hydrogen absorption mechanism in aluminium under humid conditions [10].

The presence of hydrogen in these trapping sites can cause various detrimental effects. It can create internal pressure within the material, which leads to cracking. Thus, hydrogen can also weaken the atomic bonds within the material's crystal lattice, reducing its mechanical strength and ductility [173]. The weakening of the material's structure can make it more brittle and susceptible to cracking, even under relatively low-stress conditions. This embrittlement phenomenon can initiate and propagate cracks within the aluminium alloy, reducing fatigue strength and life [174].

The identified mechanisms highlight material responses in coastal environments, including oxide layers, crack closure, phase particle edge spaces, crack propagation paths,

corrosion fatigue interactions, moisture-assisted crack propagation, and hydrogen embrittlement. These mechanisms serve as key parameters and fill a gap in the existing knowledge on the influences of temperature and humidity on aluminium structures under coastal conditions. A systematic study of these failure mechanisms can provide a scientific understanding of the complex interactions between temperature and humidity and their impact on the structural integrity of aluminium materials under coastal conditions.

Hydrogen embrittlement occurs when hydrogen atoms seep into a material, increasing brittleness and susceptibility to failure. In aluminium alloys exposed to corrosive environments, hydrogen can accumulate at defects, weakening atomic bonds, reducing mechanical strength, and initiating cracks, ultimately diminishing fatigue strength and life.

## 5. Modelling and Predictive Approaches

Modelling and prediction methods for estimating fracture toughness and fatigue crack growth of aluminium alloy typically often use a variety of techniques, including empirical modelling [175] and simulations by using finite element analysis (FEA) [176,177]. These methods are needed to characterise the fracture behaviour of aluminium alloys and ensure their safe and effective use in various applications [178,179]. It is difficult to predict how materials would fracture when exposed to various coastal environmental conditions like temperature, humidity, and corrosion. Conventional modelling tools do not help much with this process.

However, under stable crack growth, the Paris equation can become a valuable tool for predicting fatigue crack growth rate (FCGR) even in corrosive environments [53,180,181]. The relationship between temperature humidity and its effect on fracture toughness, FCGR, and fatigue life estimation has yet to be fully understood. Empirical modelling will be one method to build models for predicting fracture toughness, fatigue crack growth parameters, and fatigue life cycles of materials in coastal environments.

Curve fitting is used in material fracture behaviour analysis to predict fracture toughness and fatigue life. The effect of curve fitting on the failure probability, crack size, and fracture toughness of a failed component depends strongly on the type of distribution assumed and the quality of the fit [182]. In this method, the parameters of the curve are adjusted until they substantially match the experimental data. Once a suitable curve is created, it can predict material behaviour under various conditions. Curve fitting is often used when a simplified mathematical representation of a complex relationship is required.

The empirical modelling approach through curve fitting involves conducting experiments under controlled conditions. During these experiments, data were collected on fracture toughness, fatigue crack growth parameters, and fatigue life cycle. These experimental data are then analysed to develop empirical models describing the relationships between material properties, specific factors, and their levels [176]. Many authors [23,24,183] developed equations for predicting fracture behaviour using regression methods, a type of empirical modelling technique that involves fitting mathematical models to the experimental data to describe the relationships between corrosive environment variables.

Hassan et al. [184] used optimized neural networks to predict the fatigue crack growth rate (FCG) guided by the mutation-guided algorithm (MLA). Daniel Kovalov et al. [185] studied the corrosion fatigue of aluminium alloy 2024-T351 and found the effects of electrochemical potential, NaCl concentration, loading frequency, and temperature. Zhang T et al. [186] developed a model considering the corrosion and fatigue cycle effects of aluminium alloy 2024-T4. They used curve fitting techniques to relate the corrosion time and depth of aluminium alloys. The result of the relationship between the corrosion depth of the fatigue crack tip ( $d$ , mm) and the obtained corrosion time ( $t$ , h) is an exponential fit given by Equation (13), with a correlation coefficient of  $R^2 = 0.949$ .

$$d = 0.00981t^{0.39159} \quad (13)$$

Yichen et al. [136] used the curve fitting technique to correlate the stress range ( $s$ , Mpa) and life cycles ( $N$ ), mentioned in Equation (14), and the linear fitting was obtained with  $R^2 = 0.797$ .

$$s = 233.4906 - 12.7622\log(N) \quad (14)$$

Bergner et al. [187] used the curve fitting technique to correlate Paris constants  $C$  and  $m$  and obtained the linear fit with  $R^2 = 0.96$ . Alqahtani et al. [188] utilised the curve fitting method to find the Paris constants  $C$  and  $m$  from the Paris equation for different temperature and humidity conditions. The regression equations obtained by curve fitting were linear for fatigue life cycles and  $C$ .

Mohammad Khan et al. [189] proposed the Khan–He model, which is more suitable for experimental crack depth and frequency data at different temperatures than the established Ostachowicz model. Yang Yali et al. [190] used a curve-fitting method to predict fatigue life from surface roughness. The results demonstrated a correlation between surface roughness and fatigue life ( $N_i$ ) and found that a cubic polynomial equation provided the best fit shown in Equations (15) and (16).

$$K_t = 0.93 + 0.37b - 0.04b^2 - 0.07b\left(\frac{a}{b}\right) + 0.02\left(\frac{a}{b}\right)^2 + 0.002b^3 + 0.004b^2\left(\frac{a}{b}\right) + 0.006b\left(\frac{a}{b}\right)^2 - 0.003\left(\frac{a}{b}\right)^3 \quad (15)$$

where  $a$  and  $b$  are single micro-notch parameters, and  $K_t$  is the stress concentration factor.

$$N_i = 3.53 \times 10^{13} \left[ (207.25K_t)^{1.84} - 127^{1.84} \right]^{-2} \quad (16)$$

The calculated fatigue life values were compared to experimental results, revealing a maximum error of 15.65%. This suggests that the formulated equation obtained from curve fitting is reasonable and effective in predicting fatigue life.

These findings show the flexibility and efficiency of curve fitting techniques in developing the relationship between various parameters, aiding in understanding materials' behaviour under any conditions.

Although various models [185,186,191] are used to analyse the obtained data and predict the life cycle in non-corrosive and corrosive conditions, the current understanding still needs to consider the specific effects of temperature and humidity. Investigating how temperature and humidity interact to affect fracture toughness and FCGR behaviour is critical to ensure aluminium alloy components' reliable and safe performance in coastal environments. The effects of humidity [192,193] and temperature [48,194–196] on the fatigue properties of materials [197–200] were independently studied in earlier research. For the purpose of forecasting fatigue life and creating empirical equations for predicting and associating FCGR with fracture toughness, a thorough understanding of the combined effects of these components is essential.

Simulation techniques involve using computer-based models to replicate the behaviour of materials under various coastal environmental scenarios [201]. Finite element simulations are a standard tool used for this purpose [202,203]. In FEA, the material and environmental conditions are mathematically modelled and the simulation predicts how the material will behave. By altering the input parameters, such as temperature and humidity levels, researchers can assess their impact on fracture toughness, fatigue crack growth, and fatigue life.

Figure 20a depicts an FE simulation model of the CT specimen used in fracture toughness tests. In the contour plot, Figure 20b, the distribution of Von Mises stress in the deformed CT specimen can be observed as simulated by the FEM analysis [204]. Along with the stress distribution, fracture toughness, and fatigue life cycles, FCGR can also be predicted using commercially available simulation software.

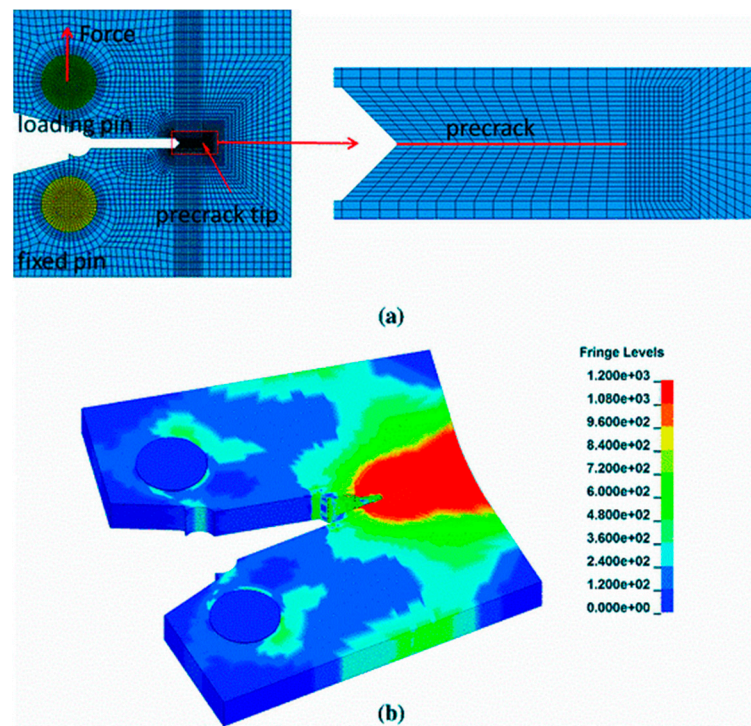


**Figure 20.** (a) Simulation model of the CT specimen for fracture toughness tests. (b) Stress distribution. Adapted from ref. [204].

Table 2 provides an overview of the various models used to predict the fracture behaviour of aluminium alloys, along with their respective methods, applications, and limitations. However, some models focus on predicting fracture behaviour under conditions including only corrosion, temperature, or humidity. Still, the combined effects of temperature and humidity in coastal environments remain unexplored. Structures in coastal areas are frequently exposed to temperature, humidity, and corrosion.

**Table 2.** Models used to predict the fracture behaviour of the aluminium alloys.

Author	Model Used	Methodology	Application	Limitation
Zhiying et al. (2016) [205]	Corrosion–fatigue	Paris model and Trantina–Johnson model	Accurate results in corrosion conditions	Does not consider the temperature and humidity
C.Q. Wang et al. (2023) [53]	Corrosion–fatigue	Trantina–Johnson model		
Huang et al. (2016) [206]	Pre-corrosion fatigue	Equivalent crack size (ECS) models and experiment	It focuses on single and multi-crack initiations	Pre-corrosion; does not consider the temperature and humidity
Ping et al. (2016) [207]	Theoretical model and numerical simulation	Pitting corrosion model	Fatigue damage was evaluated for the model of pit growth	Does not consider the temperature and humidity
Safyari et al. (2021) [107] and (2023) [208]	Humidity model	Hydrogen embrittlement mechanism	Hydrogen sensitivity index	Does not consider the temperature and corrosion
Delshad et al. (2020) [209]	Temperature model	Ductility and Yielding	Mechanical properties	Does not consider the humidity and corrosion
Mouritz et al. (2012) [210]	Temperature model	Fracture toughness	Aerospace materials	Does not consider the humidity and corrosion

Table 2. Cont.

Author	Model Used	Methodology	Application	Limitation
Kimberly et al. (2020) [108]	Temperature and corrosion model	Pitting corrosion	Mg <sub>2</sub> Si intermetallic formation	Does not consider the humidity conditions
Sarah et al. (2023) [99]	Atmospheric corrosion	Frequency and salinity, atmospheric conditions	Atmospheric corrosion FCGR	Does not consider the Temperature and humidity

## 6. Conclusions

Coastal areas present unique challenges for materials and structures. A comprehensive understanding of the material's fracture behaviour under such conditions is essential. This literature study investigates various fracture mechanisms under corrosive conditions and the interaction between corrosion, temperature, humidity, and material characteristics. Temperature and humidity influence the fatigue and fracture behaviour of materials and structures, a significant concern in engineering applications. The exposure of structures to high temperature and humidity conditions can change material properties and affect crack propagation.

Coastal environments face unique challenges due to saltwater exposure, humidity, temperature fluctuations, and corrosive agents. Saltwater accelerates material corrosion, while humidity can cause moisture absorption and deterioration. Temperature and humidity variations can affect the corrosion process. Many elements and processes can contribute to fracture mechanisms, such as corrosion fatigue, hydrogen embrittlement, and moisture-assisted crack propagation. These factors play an important role in material degradation in corrosive environments.

The existing literature has not yet provided sufficient explanations about the fatigue and fracture behaviour of the materials under temperature and humidity conditions across the structure. The following conclusions were drawn from the existing literature:

- Aluminium alloys, especially the Al6000 series, are prone to corrosion in NaCl solutions, leading to reduced fracture toughness and corrosion fatigue under cyclic loading. Elevated temperatures exceeding 70 °C impact aircraft component performance, causing microscopic cracks and corrosion pits. Pitting corrosion is observed between 20 to 80 °C, decreasing above 70 °C with the formation of an aluminium oxide layer. Research on the aluminium alloy shows a reduction in corrosion pits with rising temperatures, emphasizing the correlation between temperature and the diffusion coefficient for protective oxide layer growth.
- Humidity significantly accelerates corrosion and affects mechanical properties in coastal areas, causing surface degradation and fatigue failure. Common corrosion types include intergranular and pitting corrosion. Cyclic loading in humid air increases fracture growth rates, and hydrogen embrittlement mechanisms involve water vapor reactions leading to hydrogen absorption.

Understanding the combined effects of temperature, humidity, and corrosive marine atmospheres is crucial for addressing challenges to aluminium alloy performance in coastal environments. Addressing coastal challenges for aluminium alloys requires a deeper understanding of corrosion mechanisms, comprehensive field studies, and accurate predictive models. Exploring emerging materials and coatings tailored to coastal conditions holds promise for effective mitigation in the future.

**Author Contributions:** Writing—original draft, writing—review and editing, information collection, modifications, validation, resources, I.A.; review, modifications, supervision, A.S.; conceptualization, methodology, review, supervision, M.K. All authors have read and agreed to the published version of the manuscript.

**Funding:** This research received no external funding.

**Conflicts of Interest:** The authors declare no conflict of interest.

## References

- Mohammed, Y. Abdellah Ductile Fracture and S–N Curve Simulation of a 7075-T6 Aluminum Alloy under Static and Constant Low-Cycle Fatigue. *J. Fail. Anal. Prev.* **2021**, *21*, 1476–1488. [[CrossRef](#)]
- Salam, I.; Muhammad, W.; Ejaz, N. Fatigue Crack Growth in an Aluminum Alloy-Fractographic Study. In Proceedings of the IOP Conference Series: Materials Science and Engineering, Volume 146, 14th International Symposium on Advanced Materials, Islamabad, Pakistan, 12–16 October 2015; National Centre for Physics: Islamabad, Pakistan, 2016.
- Menan, F.; Henaff, G. Influence of Frequency and Exposure to a Saline Solution on the Corrosion Fatigue Crack Growth Behavior of the Aluminum Alloy 2024. *Int. J. Fatigue* **2009**, *31*, 1684–1695. [[CrossRef](#)]
- Abdellah, M.Y.; Alharthi, H. Fracture Toughness and Fatigue Crack Growth Analyses on a Biomedical Ti-27Nb Alloy under Constant Amplitude Loading Using Extended Finite Element Modelling. *Materials* **2023**, *16*, 4467. [[CrossRef](#)]
- Kamal, A.-S.H.; Ghazaly, N.M.; Abdellah, M.Y.; Seleem, A.-E.H.A.; Abdel-Jaber, G. Influence Parameters on the Essential Work of Fracture of 5754-H111 Aluminum Alloy Plate: Comparative Study. *SVU-Int. J. Eng. Sci. Appl.* **2023**, *4*, 243–259. [[CrossRef](#)]
- Abdellah, M.Y.; Ghazaly, N.M.; Kamal, A.-S.H.; Hagag, A.-E.; Seleem, A.; Abdel-Jaber, G. Ductile Fracture Toughness of Al 5754-H111 Alloy Using Essential Work of Fracture Method. *AIMS Mater. Sci.* **2023**, *10*, 370–389. [[CrossRef](#)]
- Abdellah, M.Y.; Fadhl, B.M.; Abu El-Ainin, H.M.; Hassan, M.K.; Backar, A.H.; Mohamed, A.F. Experimental Evaluation of Mechanical and Tribological Properties of Segregated Al-Mg-Si Alloy Filled with Alumina and Silicon Carbide through Different Types of Casting Molds. *Metals* **2023**, *13*, 316. [[CrossRef](#)]
- Doddamani, S.; Kaleemulla, M. Effect of Graphite on Fracture Toughness of 6061Al-Graphite. *Strength Fract. Complex.* **2018**, *11*, 295–308. [[CrossRef](#)]
- Igwemezie, V.; Mehmanparast, A. Waveform and Frequency Effects on Corrosion-Fatigue Crack Growth Behaviour in Modern Marine Steels. *Int. J. Fatigue* **2020**, *134*, 105484. [[CrossRef](#)]
- Alqahtani, I.; Starr, A.; Khan, M. Coupled Effects of Temperature and Humidity on Fracture Toughness of Al–Mg–Si–Mn Alloy. *Materials* **2023**, *16*, 4066. [[CrossRef](#)]
- Murphy, F.A.A.; Murphy, T.P. Influence of Material Toughness on Fracture Reliability in Steel Bridges. *Natl. Acad. Sci. Transp. Res. Board* **2021**, 1–13. [[CrossRef](#)]
- Ramesh, R.S.; Santhosh Kumar, M.V.; Yasmin, B.; Doddamani, S.; Mohamed Kaleemulla, K. Fracture Toughness Investigations of AA6061-SiC Composites: Effect of Corrosion Parameters. *Mater. Chem. Phys.* **2023**, *308*, 128224. [[CrossRef](#)]
- Tenkamp, J.; Awd, M.; Siddique, S.; Starke, P.; Walther, F. Fracture–Mechanical Assessment of the Effect of Defects on the Fatigue Lifetime and Limit in Cast and Additively Manufactured Aluminum–Silicon Alloys from HCF to VHCF Regime. *Metals* **2020**, *10*, 943. [[CrossRef](#)]
- Abdellah, M.Y. Essential Work of Fracture Assessment for Thin Aluminium Strips Using Finite Element Analysis. *Eng. Fract. Mech.* **2017**, *179*, 190–202. [[CrossRef](#)]
- Saleemsab, D.; Kiran, J.O.; Kaleemulla, M.; Bakkappa, B. Fracture Toughness Testing of 6061Al-Graphite Composites Using SENB Specimens. *J. Inst. Eng. (India)-Ser. D Springer* **2019**, *100*, 195–201. [[CrossRef](#)]
- Anderson, T.L. *Fracture Mechanics—Fundamentals and Applications*, 3rd ed.; CRC Press: Boca Raton, FL, USA, 2005.
- Dowling, N.E. *Mechanical Behavior of Materials—Engineering Methods for Deformation, Fracture and Fatigue*, 4th ed.; Pearson Education Limited: Essex, UK, 2013.
- Golewski, G.L. The Phenomenon of Cracking in Cement Concretes and Reinforced Concrete Structures: The Mechanism of Cracks Formation, Causes of Their Initiation, Types and Places of Occurrence, and Methods of Detection—A Review. *Buildings* **2023**, *13*, 765. [[CrossRef](#)]
- Golewski, G.L. Fracture Performance of Cementitious Composites Based on Quaternary Blended Cements. *Materials* **2022**, *15*, 6023. [[CrossRef](#)]
- ASTME1823-10a; Standard Terminology Relating to Fatigue and Fracture Testing. ASTM: West Conshohocken, PA, USA, 2011.
- ASTME399-22; Standard Test Method for Linear-Elastic Plane Strain Fracture Toughness K<sub>Ic</sub> of Metallic Materials. ASTM: West Conshohocken, PA, USA, 2022.
- Bharath, K.N.; Saleemsab Doddamani, A.M.; Rajesh, K.M.K. Simulation of Various Fracture Models by Varying Geometrical Parameters Using Taguchi’s DOE. *Struct. Integr. Life* **2023**, *23*, 191–195.
- Dhumansure, V.; Kalyanrao, A.A.; Doddamani, S. Optimization of Process Parameters for Fracture Toughness of Al6061-Graphite Composites. *Struct. Integr. Life* **2020**, *20*, 51–55.
- Doddamani, S.; Kaleemulla, M. Comparisons of Experimental Fracture Toughness Testing Methods of Al6061–Graphite Particulate Composites. *J. Fail. Anal. Prev.* **2019**, *19*, 730–737. [[CrossRef](#)]
- Hegde, R.; Sivaram, N.M.; Ajaykumar, B.S.; Kirthan, L.J. Evaluation of Heat Treatment Effect on Fracture Behavior of Aluminum Silicon Carbide Graphite Hybrid Composite. *Int. J. Appl. Eng. Res.* **2017**, *12*, 605–610.
- Bergant, Z.; Trdan, U.; Grum, J. Effects of Laser Shock Processing on High Cycle Fatigue Crack Growth Rate and Fracture Toughness of Aluminium Alloy 6082-T651. *Int. J. Fatigue* **2016**, *87*, 444–455. [[CrossRef](#)]
- Raviraj, M.S.; Sharanaprabhu, C.M.; Mohankumar, G.C. Experimental Investigation of Effect of Specimen Thickness on Fracture Toughness of Al-TiC Composites. *Frattura ed Integrita Strutturale* **2016**, *10*, 360–368. [[CrossRef](#)]

28. Chen, C.J.; Su, M.N.; Wang, Y.H.; Deng, X.W. Experimental Research on the Fatigue Crack Growth Behaviour of Q420C. *J. Constr. Steel Res.* **2022**, *192*, 107241. [[CrossRef](#)]
29. Doddamani, S. Fracture Toughness Investigations of Al6061-Graphite Particulate Composite Using Compact Specimens. *Frattura ed Integrità Strutturale* **2017**, *41*, 484–490. [[CrossRef](#)]
30. Zhu, X.-K.; Joyce, J.A. Review of Fracture Toughness (G, K, J, CTOD, CTOA) Testing and Standardization. *Eng. Fract. Mech.* **2012**, *85*, 1–46. [[CrossRef](#)]
31. ASTM E647–13; Standard Test Method for Measurement of Fatigue Crack Growth Rates. ASTM: West Conshohocken, PA, USA, 2014; Volume 3, pp. 1–50.
32. Wanhill, R.J.H.; Bray, G.H. Fatigue Crack Growth Behavior of Aluminum–Lithium Alloys. In *Aluminum-Lithium Alloys*; Prasad, N.E., Gokhale, A.A., Wanhill, R.J.H., Eds.; Butterworth-Heinemann: Oxford, UK, 2014; pp. 381–413.
33. Lee, E.E. *Fatigue Behavior of Silicon Carbide Whisker/Aluminum Composite*; Naval Air Development Center: Warminster, PA, USA, 1988.
34. Yuan, R.; Kruzic, J.; Zhang, X.; De Jonghe, L.; Ritchie, R. Ambient to High-Temperature Fracture Toughness and Cyclic Fatigue Behavior in Al-Containing Silicon Carbide Ceramics. *Acta Mater.* **2003**, *51*, 6477–6491. [[CrossRef](#)]
35. Achutha, M.V.; Sridhara, B.K.; Budan, A. Fatigue Life Estimation of Hybrid Aluminium Matrix Composites. *Int. J. Des. Manuf. Technol.* **2008**, *2*, 14–21.
36. Uematsu, Y.; Tokaji, K.; Kawamura, M. Fatigue Behavior of SiC-Particulate-Reinforced Aluminium Alloy Composites with Different Particle Sizes at Elevated Temperatures. *Compos. Sci. Technol.* **2008**, *68*, 2785–2791. [[CrossRef](#)]
37. Myriounis, D.P.; Hasan, S.T. Fatigue and Fracture Behaviour of Al-SiCp MMC NDE by IR Detection. In Proceedings of the 18TH International Conference on Composite Materials, Jeju Island, Republic of Korea, 21–26 August 2011.
38. Huang, J.; Spowart, J.; Jones, J. The Role of Microstructural Variability on the Very High-Cycle Fatigue Behavior of Discontinuously-Reinforced Aluminum Metal Matrix Composites Using Ultrasonic Fatigue. *Int. J. Fatigue* **2010**, *32*, 1243–1254. [[CrossRef](#)]
39. Sharma, M.; Ziemian, C.; Eden, T. Fatigue Behavior of SiC Particulate Reinforced Spray-Formed 7XXX Series Al-Alloys. *Mater. Des.* **2011**, *32*, 4304–4309. [[CrossRef](#)]
40. Joadder, B.; Shit, J.; Acharyya, S.; Dhar, S. Fatigue Failure of Notched Specimen—A Strain-Life Approach. *Mater. Sci. Appl.* **2011**, *2*, 1730–1740. [[CrossRef](#)]
41. Shahani, A.; Kashani, H.M. Assessment of Equivalent Initial Flaw Size Estimation Methods in Fatigue Life Prediction Using Compact Tension Specimen Tests. *Eng. Fract. Mech.* **2013**, *99*, 48–61. [[CrossRef](#)]
42. Ciavarella, M.; D’antuono, P.; Demelio, G. Generalized Definition of “Crack-like” Notches to Finite Life and SN Curve Transition from “Crack-like” to “Blunt Notch” Behavior. *Eng. Fract. Mech.* **2017**, *179*, 154–164. [[CrossRef](#)]
43. Raposo, P.; Correia, J.A.F.O.; De Jesus, A.M.P.; Calçada, R.A.B.; Lesiuk, G.; Hebdon, M.; Fernández-Canteli, A. Probabilistic Fatigue S-N Curves Derivation for Notched Components. *Frattura ed Integrità Strutturale* **2017**, *42*, 105–118. [[CrossRef](#)]
44. Saleemsab Doddamani, M.K.K. Effect of Thickness on Fracture Toughness of Al6061-Graphite. *J. Solid Mech.* **2019**, *11*, 635–643.
45. Farheen Kulsum, A.S.D. Review on Corrosion Behavior, Fatigue Behavior and Fracture Toughness of Al Alloy MMCS. *Mater. Today Proc.* **2024**; *in press*. [[CrossRef](#)]
46. Antunes, F.V.; Serrano, S.; Branco, R.; Prates, P. Fatigue Crack Growth in the 2050-T8 Aluminium Alloy. *Int. J. Fatigue* **2018**, *115*, 79–88. [[CrossRef](#)]
47. Li, H.; Li, J.; Yuan, H. Application of a Cohesive Zone Model for Simulating Fatigue Crack Growth from Moderate to High  $\Delta K$  Levels of Inconel 718. *Int. J. Aerosp. Eng.* **2018**, *2018*, 4048386. [[CrossRef](#)]
48. Alqahtani, I.M.; Starr, A.; Khan, M. Experimental and Theoretical Aspects of Crack Assisted Failures of Metallic Alloys in Corrosive Environments—A Review. *Mater. Today Proc.* **2022**, *66*, 2530–2535. [[CrossRef](#)]
49. Niazi, H.; Eadie, R.; Chen, W.; Zhang, H. High PH Stress Corrosion Cracking Initiation and Crack Evolution in Buried Steel Pipelines: A Review. *Eng. Fail. Anal.* **2021**, *120*, 105013. [[CrossRef](#)]
50. Blanc, C.; Creus, J.; Touzet-Cortina, M. Stress Corrosion Cracking. Between the Corrosion Defect and the Long Crack: The Phase of the Initiation of the Cracks. In *Mechanics—Microstructure—Corrosion Coupling*; Christine Blanc, I.A., Ed.; Elsevier: Amsterdam, The Netherlands, 2019; pp. 287–312.
51. Alqahtani, I.; Starr, A.; Khan, M. Crack Propagation Behaviour under Corrosion and Thermomechanical Loads. In Proceedings of the 7th International Conference on Sustainable Materials and Recent Trends in Mechanical Engineering (SMARTME-2023), Bengaluru, India, 11–12 August 2023; pp. 37–45.
52. Pedferri, P. Stress Corrosion Cracking and Corrosion-Fatigue. In *Corrosion Science and Engineering*; Engineering Materials; Springer: Cham, Switzerland, 2018; pp. 243–273.
53. Wang, C.Q.; Xiong, J.J.; Sheno, R.A.; Liu, M.D.; Liu, J.Z. A Modified Model to Depict Corrosion Fatigue Crack Growth Behavior for Evaluating Residual Lives of Aluminum Alloys. *Int. J. Fatigue* **2016**, *83*, 280–287. [[CrossRef](#)]
54. Adeboye, S.A.; Adebowale, A.D.; Siyanbola, T.O.; Ajanaku, K.O. Coatings and the Environment: A Review of Problems, Progress and Prospects. In Proceedings of the IOP Conference Series: 6th International Conference on Science and Sustainable Development (ICSSD 2022), Virtual, 9–10 December 2022; Volume 1197.
55. Panda, R.; Fatma, K.; Tripathy, J. Anti-Corrosion and Anti-Wear Ceramic Coatings. In *Advanced Ceramic Coatings*; Gupta, R.K., Motallebzadeh, A., Kakooei, S., Nguyen, T.A., Behera, A., Eds.; Elsevier: Amsterdam, The Netherlands, 2023; pp. 197–217.

56. Shaikh, S. Nanomaterials Applied in Coatings: Synthesis, Structures, Properties, and Applications. *Coatings* **2022**, *12*, 1773. [[CrossRef](#)]
57. Putatunda, S.K.; Bajajand, S.; Boileau, J. A Novel Method for Determining the Fatigue Threshold and Fracture Toughness from a Single Test. *Int. J. Metall. Met. Phys.* **2018**, *3*, 1–11. [[CrossRef](#)]
58. Robertson, S.W.; Ritchie, R.O. A Fracture-Mechanics-Based Approach to Fracture Control in Biomedical Devices Manufactured from Superelastic Nitinol Tube. *J. Biomed. Mater. Res.—Part B Appl. Biomater.* **2008**, *84*, 26–33. [[CrossRef](#)] [[PubMed](#)]
59. Perez, N. *Fracture Mechanics*, 2nd ed.; Springer: Berlin/Heidelberg, Germany, 2016; ISBN 978-3-319-24997-1.
60. Saleemsab Doddamani, M.K.K. Review of Experimental Fracture Toughness (K<sub>IC</sub>) of Aluminium Alloy and Aluminium MMCs Metal Matrix Composites. *Int. J. Fract. Damage Mech.* **2016**, *2*, 38–51.
61. Lai, M.O.; Ferguson, W.G. Fracture Toughness of Aluminium Alloy 7075-T6 in the as-Cast Condition. *Mater. Sci. Eng.* **1985**, *74*, 133–138. [[CrossRef](#)]
62. Hill, M.R.; Panontin, T.L. Micromechanical Modeling of Fracture Initiation in 7050 Aluminum. *Eng. Fract. Mech.* **2002**, *69*, 2163–2186. [[CrossRef](#)]
63. Urrego, L.F.; García-Beltrán, O.; Arzola, N.; Araque, O. Mechanical Fracture of Aluminium Alloy (AA 2024-T4), Used in the Manufacture of a Bioproducts Plant. *Metals* **2023**, *13*, 1134. [[CrossRef](#)]
64. Tsangarakis, N. All Modes Fracture Toughness of Two Aluminium Alloys. *Eng. Fract. Mech.* **1987**, *26*, 313–321. [[CrossRef](#)]
65. Prasad, N.E.; Kamat, S.V.; Prasad, K.S.; Malakondaiah, G.; Kutumbarao, V. In-Plane Anisotropy in the Fracture Toughness of an Al-Li 8090 Alloy Plate. *Eng. Fract. Mech.* **1993**, *46*, 209–223. [[CrossRef](#)]
66. Alrashed, F.; Asif, M. Climatic Classifications of Saudi Arabia for Building Energy Modelling. *Energy Procedia* **2015**, *75*, 1425–1430. [[CrossRef](#)]
67. Alqahtani, I.M.; Starr, A.; Khana, M. Fracture Toughness Investigation of AL6082-T651 Alloy under Corrosive Environmental Conditions. In Proceedings of the 11th International Conference on Fracture Fatigue and Wear (FFW-2023), Ghent, Belgium, 29–31 August 2023.
68. Tang, Y.; Meng, Q.; Ren, P. Spatial Distribution and Concentrations of Salt Fogs in a Coastal Urban Environment: A Case Study in Zhuhai City. *Build. Environ.* **2023**, *234*, 110156. [[CrossRef](#)]
69. Loader, P.B.C. *Effect of High Temperature Exposure on the Mechanical Properties of Cold Expanded Open Holes in 7050-T7451 Aluminium Alloy*; Defence Science and Technology Organisation: Edinburgh, Australia, 2008.
70. Cavalcante, T.R.F.; Pereira, G.S.; Koga, G.Y.; Bolfarini, C.; Bose Filho, W.W.; Avila, J.A. Fatigue Crack Propagation of Aeronautic AA7050-T7451 and AA2050-T84 Aluminum Alloys in Air and Saline Environments. *Int. J. Fatigue* **2022**, *154*, 106519. [[CrossRef](#)]
71. Zheng, Y.Y.; Luo, B.H.; He, C.; Gao, Y.; Bai, Z.H. Corrosion Evolution and Behaviour of Al–2.1Mg–1.6Si Alloy in Chloride Media. *Rare Met.* **2021**, *40*, 908–919. [[CrossRef](#)]
72. Zakaria, H.M. Microstructural and Corrosion Behavior of Al/SiC Metal Matrix Composites. *Ain Shams Eng. J.* **2014**, *5*, 831–838. [[CrossRef](#)]
73. Cai, Y.; Xu, Y.; Zhao, Y.; Zhang, W.; Yao, J.; Wei, M.; Zhou, K.; Ma, X. Quantitative Understanding of the Environmental Effect on B10 Copper Alloy Corrosion in Seawater. *Metals* **2021**, *11*, 1080. [[CrossRef](#)]
74. Little, B.J.; Ray, R.I.; Lee, J. Understanding Marine Biocorrosion: Experiments with Artificial and Natural Seawater. In *Understanding Biocorrosion*; Liengen, T., Féron, D., Basséguy, R., Beech, I.B., Eds.; Woodhead Publishing: Sawston, UK, 2014; pp. 329–340.
75. Zai, B.A.; Khan, M.A.; Khan, K.A.; Mansoor, A.; Shah, A.; Shahzad, M. The Role of Dynamic Response Parameters in Damage Prediction. *Proc. Inst. Mech. Eng. Part C J. Mech. Eng. Sci.* **2019**, *233*, 4620–4636. [[CrossRef](#)]
76. Sarah Galyon Dorman, S.A.F. Examination of the Effects of Specimen Geometry on Single Edge-Cracked Tension Specimens. *Eng. Fract. Mech.* **2019**, *209*, 221–227. [[CrossRef](#)]
77. Ramsden, E. Development Tools. In *Hall-Effect Sensors*; Ramsden, E., Ed.; Newnes: Oxford, UK, 2006; pp. 187–202. ISBN 9780750679343.
78. Darehshouri, S.; Michelsen, N.; Schüth, C.; Schulz, S. A Low-Cost Environmental Chamber to Simulate Warm Climatic Conditions. *Vadose Zone J.* **2020**, *19*, e20023. [[CrossRef](#)]
79. Kurniawan, I.; Faridah; Utami, S.S. Characterizing of Climate Chamber Thermal Environment Using the CFD Simulation Method Using IES VE. *AIP Conf. Proc.* **2020**, *2223*, 050010. [[CrossRef](#)]
80. Czerwinski, F. Thermal Stability of Aluminum Alloys. *Materials* **2020**, *13*, 3441. [[CrossRef](#)] [[PubMed](#)]
81. Aboura, Y.; Garner, A.; Euesden, R.; Barrett, Z.; Engel, C.; Holroyd, N.; Prangnell, P.; Burnett, T. Understanding the Environmentally Assisted Cracking (EAC) Initiation and Propagation of New Generation 7xxx Alloys Using Slow Strain Rate Testing. *Corros. Sci.* **2022**, *199*, 110161. [[CrossRef](#)]
82. Brown, M.D. *Moisture Absorption and Desorption Effects on Mechanical Behavior in Specialty Polyamide Products*; Lehigh University: Bethlehem, PA, USA, 2019.
83. Yadav, V.; Gaur, V.; Singh, I. Corrosion-Fatigue Behavior of Welded Aluminum Alloy 2024-T3. *Int. J. Fatigue* **2023**, *173*, 107675. [[CrossRef](#)]
84. Gyarmati, G.; Bubonyi, T.; Fegyverneki, G.; Tokár, M.; Mende, T. Interactions of Primary Intermetallic Compound Particles and Double Oxide Films in Liquid Aluminum Alloys. *Intermetallics* **2022**, *149*, 107681. [[CrossRef](#)]
85. Liu, Y.; Kang, S.; Kim, H. The Complex Microstructures in an As-Cast Al–Mg–Si Alloy. *Mater. Lett.* **1999**, *41*, 267–272. [[CrossRef](#)]

86. Eckermann, F.; Suter, T.; Uggowitzner, P.J.; Afseth, A.; Schmutz, P. The Influence of MgSi Particle Reactivity and Dissolution Processes on Corrosion in Al-Mg-Si Alloys. *Electrochim. Acta* **2008**, *54*, 844–855. [CrossRef]
87. Wei, Z.; Goehring, T.; Mioduszewski, M.; Luo, L.; Kotrba, A.; Rybarz, M.; Ellinghaus, K.; Pieszkalla, M. Failure Mechanisms and Modes Analysis of Vehicle Exhaust Components and Systems. In *Handbook of Materials Failure Analysis with Case Studies from the Aerospace and Automotive Industries*; Abdel Salam Hamdy Makhlouf, M.A., Ed.; Butterworth-Heinemann: Oxford, UK, 2016; pp. 393–432.
88. Peng, C.; Cao, G.; Gu, T.; Wang, C.; Wang, Z.; Sun, C. The Corrosion Behavior of the 6061 Al Alloy in Simulated Nansha Marine Atmosphere. *J. Mater. Res. Technol.* **2022**, *19*, 709–721. [CrossRef]
89. Noell, P.J.; Karasz, E.; Schindelholz, E.J.; Polonsky, A.T.; Campbell, I.; Katona, R.M.; Melia, M.A. The Evolution of Pit Morphology and Growth Kinetics in Aluminum during Atmospheric Corrosion. *npj Mater. Degrad.* **2023**, *7*, 12. [CrossRef]
90. Cao, M.; Liu, L.; Fan, L.; Yu, Z.; Li, Y.; Oguzie, E.E.; Wang, F. Influence of Temperature on Corrosion Behavior of 2A02 Al Alloy in Marine Atmospheric Environments. *Materials* **2018**, *11*, 235. [CrossRef]
91. Amura, M.; Aiello, L.; Colavita, M.; De Paolis, F.; Bernabei, M. Failure of a Helicopter Main Rotor Blade. *Procedia Mater. Sci.* **2014**, *3*, 726–731. [CrossRef]
92. Romeyn, A. *Main Rotor Blade Failure Analysis Report*; IOP Publishing: Philadelphia, PA, USA, 2005.
93. Sunrise Helicopters Inc., Canada. In-Flight Separation of Main Rotor Blade and Collision with Terrain. 2011. Available online: <https://www.bst-tsb.gc.ca/eng/rappports-reports/aviation/2011/a11o0205/a11o0205.pdf> (accessed on 1 March 2024).
94. Cicolin, D.; Trueba, M.; Trasatti, S. Effect of Chloride Concentration, PH and Dissolved Oxygen, on the Repassivation of 6082-T6 Al Alloy. *Electrochim. Acta* **2014**, *124*, 27–35. [CrossRef]
95. Otieno, M.; Thomas, M. Marine Exposure Environments and Marine Exposure Sites. In *Marine Concrete Structures*; Alexander, M.G., Ed.; Woodhead Publishing: Sawston, UK, 2016; pp. 171–196.
96. Vargel, C. Chapter D.1—Freshwater. In *Corrosion of Aluminium*; Vargel, C., Ed.; Elsevier: Amsterdam, The Netherlands, 2004; pp. 299–327. ISBN 9780080444956.
97. Tao, J.; Xiang, L.; Zhang, Y.; Zhao, Z.; Su, Y.; Chen, Q.; Sun, J.; Huang, B.; Peng, F. Corrosion Behavior and Mechanical Performance of 7085 Aluminum Alloy in a Humid and Hot Marine Atmosphere. *Materials* **2022**, *15*, 7503. [CrossRef]
98. Luo, D.; Li, F.; Xing, G. Corrosion Resistance of 6061-T6 Aluminium Alloy and Its Feasibility of near-Surface Reinforcements in Concrete Structure. *Rev. Adv. Mater. Sci.* **2022**, *61*, 638–653. [CrossRef]
99. Free, B.; Marino, G.; Schindelholz, E.; Galyon Dorman, S.; (Warner) Locke, J.S. Measurement of Atmospheric Corrosion Fatigue Crack Growth Rates on AA7085-T7451. *Int. J. Fatigue* **2023**, *167*, 107368. [CrossRef]
100. Mao, Y.; Zhu, Y.; Deng, C.-M.; Sun, S.; Xia, D.-H. Analysis of Localized Corrosion Mechanism of 2024 Aluminum Alloy at a Simulated Marine Splash Zone. *Eng. Fail. Anal.* **2022**, *142*, 106759. [CrossRef]
101. Bray, G.H.; Bucci, R.J.; Brazill, R.L. Lessons Neglected: Effects of Moist Air on Fatigue and Fatigue Crack Growth in Aluminum Alloys. *Mater. Sci. Forum* **2000**, *331–337*, 1413–1426.
102. Ahmad, Z. Chapter 10—Atmospheric Corrosion. In *Principles of Corrosion Engineering and Corrosion Control*; Butterworth-Heinemann: Oxford, UK, 2006; pp. 550–575. ISBN 9780750659246.
103. Bradshaw, F.J.; Wheeler, C. The Influence of Gaseous Environment and Fatigue Frequency on the Growth of Fatigue Cracks in Some Aluminium Alloys. *Int. J. Fract. Mech.* **1969**, *5*, 255–268. [CrossRef]
104. Davidson, D.L.; Lankford, J. The Effect of Water Vapor on Fatigue Crack Tip Mechanics in 7075-T651 Aluminium Alloy. *Fatigue Fract. Eng. Mater. Struct.* **1983**, *6*, 241–256. [CrossRef]
105. Holper, B.; Mayer, H.; Vasudevan, A.; Stanzi-Tschegg, S. Near Threshold Fatigue Crack Growth in Aluminium Alloys at Low and Ultrasonic Frequency: Influences of Specimen Thickness, Strain Rate, Slip Behaviour and Air Humidity. *Int. J. Fatigue* **2003**, *25*, 397–411. [CrossRef]
106. Young, G.A.; Scully, J.R. The Effects of Test Temperature, Temper, and Alloyed Copper on the Hydrogen-Controlled Crack Growth Rate of an Al-Zn-Mg-(Cu) Alloy. *Met. Mater. Trans. A* **2002**, *33*, 1167–1181. [CrossRef]
107. Safyari, M.; Hojo, T.; Moshtaghi, M. Effect of Environmental Relative Humidity on Hydrogen-Induced Mechanical Degradation in an Al-Zn-Mg-Cu Alloy. *Vacuum* **2021**, *192*, 110489. [CrossRef]
108. L'haridon-Quaireau, S.; Laot, M.; Colas, K.; Kapusta, B.; Delpéch, S.; Gosset, D. Effects of Temperature and PH on Uniform and Pitting Corrosion of Aluminium Alloy 6061-T6 and Characterisation of the Hydroxide Layers. *J. Alloys Compd.* **2020**, *833*, 155146. [CrossRef]
109. Khodor, J.; Özenç, K.; Lin, G.; Kaliske, M. Characterization of Fatigue Crack Growth by Cyclic Material Forces. *Eng. Fract. Mech.* **2021**, *243*, 107514. [CrossRef]
110. González-Velázquez, J. Environmentally-Assisted Fracture. In *Fractography and Failure Analysis. Structural Integrity*; Springer: Cham, Switzerland, 2018.
111. Navidrad, M.; Stepniowski, W.J.; Cartier, E.; Christ, T.; Watanabe, M.; Misiolek, W.Z. Investigation on the Strain Induced Oxide Layer Fracture and Bonding During Cold Rolling of Aluminum Alloys. In *The Minerals, Metals & Materials Series*; Daehn, G., Cao, J., Kinsey, B., Tekkaya, E.V., Eds.; Springer: Cham, Switzerland, 2021.
112. Song, H.; Liu, C.; Zhang, H.; Leen, S.B. A DIC-Based Study on Fatigue Damage Evolution in Pre-Corroded Aluminum Alloy 2024-T4. *Materials* **2018**, *11*, 2243. [CrossRef]

113. Pu, J.; Zhang, Y.; Zhang, X.; Yuan, X.; Ren, P.; Jin, Z. Mapping the Fretting Corrosion Behaviors of 6082 Aluminum Alloy in 3.5% NaCl Solution. *Wear* **2021**, *482–483*, 203975. [CrossRef]
114. Chugh, B.; Taraphdar, P.K.; Biswal, H.J.; Devi, N.R.; Dorothy, R.; Manimaran, N.; Rajendran, S. Corrosion Inhibition by Aluminum Oxide. In *Inorganic Anticorrosive Materials*; Verma, C., Aslam, J., Hussain, C.M.I., Eds.; Elsevier: Amsterdam, The Netherlands, 2022; pp. 231–249.
115. Wang, D.; Yang, D.; Zhang, D.; Li, K.; Gao, L.; Lin, T. Electrochemical and DFT Studies of Quinoline Derivatives on Corrosion Inhibition of AA5052 Aluminium Alloy in NaCl Solution. *Appl. Surf. Sci.* **2015**, *357*, 2176–2183. [CrossRef]
116. Vargel, C. Oxides and Peroxides. In *Corrosion of Aluminium*; Vargel, C., Ed.; Elsevier: Amsterdam, The Netherlands, 2004; pp. 357–365.
117. Dias, C.; Ventura, J. Understanding the Influence of Metal Oxide Layer Thickness and Defects on Resistive Switching Behavior Through Numerical Modeling. *Phys. Status Solidi A-Appl. Mater. Sci.* **2022**, *220*, 202200730. [CrossRef]
118. Cao, Y.; Xu, H.; Zhan, J.; Zhang, H.; Cui, S.; Tang, W. Microstructure, Growth Kinetics and Formation Mechanism of Oxide Layers on AlN Ceramic Substrates. *J. Ceram. Sci. Technol.* **2018**, *9*, 263–270. [CrossRef]
119. Cao, X.; Campbell, J. Oxide Inclusion Defects in Al-Si-Mg Cast Alloys. *Can. Metall. Q.* **2005**, *44*, 435–448. [CrossRef]
120. Pokorný, P.; Vojtek, T.; Jambor, M.; Náhlik, L.; Hutař, P. Effect of Underload Cycles on Oxide-Induced Crack Closure Development in Cr-Mo Low-Alloy Steel. *Materials* **2021**, *14*, 2530. [CrossRef]
121. Yamada, Y.; Newman, J.C. Crack-Closure Behavior of 2324-T39 Aluminum Alloy near-Threshold Conditions for High Load Ratio and Constant K<sub>max</sub> Tests. *Int. J. Fatigue* **2009**, *31*, 1780–1787. [CrossRef]
122. Casperson, M.C.; Carroll, J.D.; Lambros, J.; Sehitoglu, H.; Dodds, R.H. Investigation of Thermal Effects on Fatigue Crack Closure Using Multiscale Digital Image Correlation Experiments. *Int. J. Fatigue* **2014**, *61*, 10–20. [CrossRef]
123. Pippan, R.; Hohenwarter, A. Fatigue Crack Closure: A Review of the Physical Phenomena. *Fatigue Fract. Eng. Mater. Struct.* **2017**, *40*, 471–495. [CrossRef]
124. Culliton, D.; Betts, A.J.; Kennedy, D. Impact of Intermetallic Precipitates on the Tribological and/or Corrosion Performance of Cast Aluminium Alloys: A Short Review. *Int. J. Cast Met. Res.* **2013**, *26*, 65–71. [CrossRef]
125. Koleva, D.A.; Hu, J.; Stroeven, P. Microstructure Alterations Underlying Electrochemical Process of Chloride-Induced Corrosion. In *Brittle Matrix Composites 8*; Brandt, A.M., Li, V.C., Marshall, I.H., Eds.; Woodhead Publishing: Sawston, UK, 2006; pp. 571–580.
126. Shrivastava, V.; Dubey, S.; Gupta, G.K.; Singh, I.B. Influence of Alpha Nanoalumina Reinforcement Content on the Microstructure, Mechanical and Corrosion Properties of Al6061-Al<sub>2</sub>O<sub>3</sub> Composite. *J. Mater. Eng. Perform.* **2017**, *26*, 4424–4433. [CrossRef]
127. Kciuk, M.; Kurc, A.; Szewczenko, J. Structure and Corrosion Resistance of Aluminium AlMg2.5; AlMg5Mn and AlZn5Mg1 Alloys. *J. Achiev. Mater. Manuf. Eng.* **2010**, *41*, 74–81.
128. Zhu, Y.; Sun, K.; Frankel, G.S. Intermetallic Phases in Aluminum Alloys and Their Roles in Localized Corrosion. *J. Electrochem. Soc.* **2018**, *165*, C807–C820. [CrossRef]
129. Zarif, M.; Spacil, I.; Pabel, T.; Schumacher, P.; Li, J. Effect of Ca and P on the Size and Morphology of Eutectic Mg<sub>2</sub>Si in High-Purity Al-Mg-Si Alloys. *Metals* **2023**, *13*, 784. [CrossRef]
130. Blau, P.J. Elevated-Temperature Tribology of Metallic Materials. *Tribol. Int.* **2010**, *43*, 1203–1208. [CrossRef]
131. Gain, A.K.; Zhang, L. Temperature and Humidity Effects on Microstructure and Mechanical Properties of an Environmentally Friendly Sn–Ag–Cu Material. *J. Mater. Sci.* **2019**, *54*, 12863–12874. [CrossRef]
132. Arrabal, R.; Pardo, A.; Merino, M.C.; Merino, S.; Mohedano, M.; Casajús, P. Corrosion Behaviour of Mg/Al Alloys in High Humidity Atmospheres. *Mater. Corros. Und. Korros.* **2011**, *62*, 326–334. [CrossRef]
133. Shyam, A.; Lara-Curzio, E. A Model for the Formation of Fatigue Striations and Its Relationship with Small Fatigue Crack Growth in an Aluminum Alloy. *Int. J. Fatigue* **2010**, *32*, 1843–1852. [CrossRef]
134. Laird, C. The Influence of Metallurgical Structure on the Mechanisms of Fatigue Crack Propagation. *ASTM STP 415 Am. Soc. Test. Mats* **1967**, *131*, 1–10.
135. Data, F.M. Linear Elastic Fracture Mechanics (LEFM): Part Two. Available online: <https://www.totalmateria.com/page.aspx?ID=CheckArticle&site=kts&LN=IT&NM=299> (accessed on 3 September 2023).
136. Liu, Y.; Pan, Q.; Liu, B.; Yu, Q.; Li, G.; Pan, D. Effect of Aging Treatments on Fatigue Properties of 6005A Aluminum Alloy Containing Sc. *Int. J. Fatigue* **2022**, *163*, 107103. [CrossRef]
137. Zhu, M.; Yang, S.; Bai, Y.; Fan, C. Microstructure and Fatigue Damage Mechanism of 6082-T6 Aluminium Alloy Welded Joint. *Mater. Res. Express* **2021**, *8*, 056505. [CrossRef]
138. Anis, S.F.; Koyama, M.; Hamada, S.; Noguchi, H. Mode I Fatigue Crack Growth Induced by Strain-Aging in Precipitation-Hardened Aluminum Alloys. *Theor. Appl. Fract. Mech.* **2019**, *104*, 102340. [CrossRef]
139. Ma, L.; Liu, C.; Ma, M.; Wang, Z.; Wu, D.; Liu, L.; Song, M. Fatigue Fracture Analysis on 2524 Aluminum Alloy with the Influence of Creep-Aging Forming Processes. *Materials* **2022**, *15*, 3244. [CrossRef]
140. Doré, M.J.; Maddox, S.J. Accelerated Fatigue Crack Growth in 6082 T651 Aluminium Alloy Subjected to Periodic Underloads. *Procedia Eng.* **2013**, *66*, 313–322. [CrossRef]
141. Sharma, V.M.J.; Sree Kumar, K.; Nageswara Rao, B.; Pathak, S.D. Effect of Aging Treatments on the Fatigue Crack Growth and Threshold Behavior of AA 2219 Aluminium Alloy. *Trans. Indian Inst. Met.* **2010**, *63*, 535–540. [CrossRef]
142. Chapetti, M.D.; Gubeljak, N.; Kozak, D. Intrinsic Fatigue Limit and the Minimum Fatigue Crack Growth Threshold. *Materials* **2023**, *16*, 5874. [CrossRef]

143. Mathieu, F.; Hild, F.; Roux, S. Identification of a Crack Propagation Law by Digital Image Correlation. *Int. J. Fatigue* **2012**, *36*, 146–154. [[CrossRef](#)]
144. Kallien, Z.; Knothe-Horstmann, C.; Klusemann, B. Fatigue Crack Propagation in AA5083 Structures Additively Manufactured via Multi-Layer Friction Surfacing. *Addit. Manuf. Lett.* **2023**, *6*, 100154. [[CrossRef](#)]
145. Belan, J.; Kuchariková, L.; Tillová, E.; Závodská, D.; Chalupová, M. Effect of Fatigue Loading Mode on 718 Alloy Fatigue Properties. *Period. Polytech. Transp. Eng.* **2019**, *47*, 335–341. [[CrossRef](#)]
146. Ma, J.; Li, D.; Du, S.; Han, Z.; Luo, P.; Zhao, J. Comparison of Subcritical Crack Growth and Dynamic Fracture Propagation in Rocks under Double-Torsion Tests. *Int. J. Rock Mech. Min. Sci.* **2023**, *170*, 105481. [[CrossRef](#)]
147. Hana, N.; Umeda, M.; Akiyoshi, M.; Mitamura, K.; Amaya, K. Crack Identification by Digital Image Correlation Method Using Crack Shape as Prior Information. *ASME J. Press. Vessel Technol.* **2023**, *145*, 041601. [[CrossRef](#)]
148. Ermakova, A.; Ganguly, S.; Razavi, N.; Berto, F.; Mehmanparast, A. Experimental Investigation of the Fatigue Crack Growth Behavior in Wire Arc Additively Manufactured ER100S-1 Steel Specimens. *Fatigue Fract. Eng. Mater. Struct.* **2022**, *45*, 371–385. [[CrossRef](#)]
149. Milella, P.P. *Fatigue and Corrosion in Metals*; Springer Science & Business Media: Berlin/Heidelberg, Germany, 2012.
150. Arzaghi, E.; Abbassi, R.; Garaniya, V.; Binns, J.; Chin, C.; Khakzad, N.; Reniers, G. Developing a Dynamic Model for Pitting and Corrosion-Fatigue Damage of Subsea Pipelines. *Ocean Eng.* **2018**, *150*, 391–396. [[CrossRef](#)]
151. Guo, Y.; Shao, Y.; Gao, X.; Li, T.; Zhong, Y.; Luo, X. Corrosion Fatigue Crack Growth of Serviced API 5L X56 Submarine Pipeline. *Ocean Eng.* **2022**, *256*, 111502. [[CrossRef](#)]
152. Gangloff, R.P. Environmental Cracking Corrosion Fatigue. In *ASTM International: West Conshohocken*; ASTM International: West Conshohocken, PA, USA, 2005; pp. 302–321.
153. Wang, Q.Y.; Pidaparti, R.M.; Palakal, M.J. Comparative Study of Corrosion-Fatigue in Aircraft Materials. *AIAA J.* **2001**, *39*, 325–330. [[CrossRef](#)]
154. Luer, K.; DuPont, J.; Marder, A.; Skelonis, C. Corrosion Fatigue of Alloy 625 Weld Claddings in Combustion Environments. *Mater. High Temp.* **2001**, *18*, 11–19. [[CrossRef](#)]
155. Muñoz, A.F.; Buenhombre, J.L.M.; García-Diez, A.I.; Fabal, C.C.; Díaz, J.J.G. Fatigue Study of the Pre-Corroded 6082-T6 Aluminum Alloy in Saline Atmosphere. *Metals* **2020**, *10*, 1260. [[CrossRef](#)]
156. Correia, J.A.F.O.; De Jesus, A.M.P.; Alves, A.S.F.; Lesiuk, G.; Tavares, P.J.S.; Moreira, P.M.G.P. Fatigue Crack Growth Behaviour of the 6082-T6 Aluminium Using CT Specimens with Distinct Notches. *Procedia Struct. Integr.* **2016**, *2*, 3272–3279. [[CrossRef](#)]
157. Alireza Behvar, M.H. A Critical Review on Very High Cycle Corrosion Fatigue: Mechanisms, Methods, Materials, and Models. *J. Space Saf. Eng.* **2023**, *10*, 284–323. [[CrossRef](#)]
158. Saintier, N.; El May, M.; Odemer, G.; Hénaff, G.; Bosch, C.; Feaugas, X.; Couvant, T. Corrosion and Hydrogen Fatigue at Different Scales. In *Mechanics—Microstructure—Corrosion Coupling*; Christine Blanc, I.A., Ed.; Elsevier: Amsterdam, The Netherlands, 2019; pp. 385–411.
159. Mudali, U.K. Materials for Hostile Corrosive Environments. In *Materials Under Extreme Conditions*; Tyagi, A.K., Banerjee, S., Eds.; Elsevier: Amsterdam, The Netherlands, 2017; pp. 91–128.
160. Gong, K.; Wu, M.; Liu, X.; Liu, G. Nucleation and Propagation of Stress Corrosion Cracks: Modeling by Cellular Automata and Finite Element Analysis. *Mater. Today Commun.* **2022**, *33*, 104886. [[CrossRef](#)]
161. Chen, W.; Lu, W.; Gou, G.; Dian, L.; Zhu, Z.; Jin, J. The Effect of Fatigue Damage on the Corrosion Fatigue Crack Growth Mechanism in A7N01P-T4 Aluminum Alloy. *Metals* **2023**, *13*, 104. [[CrossRef](#)]
162. Ge, F.; Fan, L.; Liang, J.; Pang, K.; Li, H.; Wang, X.; Cui, Z. Corrosion Evolution of High-Strength Aluminum Alloys in the Simulated Service Environment of Amphibious Aircraft in the Presence of Chloride and Bisulfite. *Acta Metall. Sin. (Engl. Lett.)* **2021**, *34*, 1679–1694. [[CrossRef](#)]
163. Mahmood, S.; Gallagher, C.; Engelberg, D.L. Atmospheric Corrosion of Aluminum Alloy 6063 Beneath Ferric Chloride Corrosion Product Droplets. *Corrosion* **2020**, *76*, 985–994. [[CrossRef](#)]
164. Kumar, P.; Verma, B.B. Propagation of Corrosion Induced Fatigue Crack in Aluminum Alloy. *AIMS Mater. Sci.* **2022**, *9*, 512–521. [[CrossRef](#)]
165. Chen, H.; Chow, C.L.; Lau, D. Deterioration Mechanisms and Advanced Inspection Technologies of Aluminum Windows. *Materials* **2022**, *15*, 354. [[CrossRef](#)]
166. Shan, J.; Hou, D.; Zhang, J.; Xin, X.; Cao, G.; Genzhe, H. Effects of the Extrusion Ratio on the Intergranular Corrosion Behaviour of 6082 Aluminium Alloy. *Mater. Corros. Und. Korros.* **2018**, *69*, 365–375. [[CrossRef](#)]
167. Nagumo, M. *Fundamentals of Hydrogen Embrittlement*, 1st ed.; Springer: Singapore, 2018.
168. Sergeev, N.N.; Sergeev, A.N.; Kutepov, S.N.; Kolmakov, A.G.; Gvozdev, A.E. Mechanism of the Hydrogen Cracking of Metals and Alloys, Part II (Review). *Inorg. Mater. Appl. Res.* **2019**, *10*, 32–41. [[CrossRef](#)]
169. Albrecht, J.; Bernstein, I.M.; Thompson, A.W. Evidence for Dislocation Transport of Hydrogen in Aluminum. *Met. Mater. Trans. A* **1982**, *13*, 811–820. [[CrossRef](#)]
170. Bochkaryova, A.V.; Li, Y.V.; Barannikova, S.A.; Zuev, L.B. The Effect of Hydrogen Embrittlement on the Mechanical Properties of Aluminum Alloy. *IOP Conf. Ser. Mater. Sci. Eng.* **2015**, *71*, 012057. [[CrossRef](#)]
171. Ambat, R.; Dwarakadasa, E.S. Effect of Hydrogen in Aluminium and Aluminium Alloys: A Review. *Bull. Mater. Sci.* **1990**, *19*, 103–114. [[CrossRef](#)]

172. Xie, D.; Li, S.; Li, M.; Wang, Z.; Gumbsch, P.; Sun, J.; Ma, E.; Li, J.; Shan, Z. Hydrogenated Vacancies Lock Dislocations in Aluminium. *Nat. Commun.* **2016**, *7*, 13341. [[CrossRef](#)] [[PubMed](#)]
173. Liang, Y.; Ahn, D.; Sofronis, P.; Dodds, R.; Bammann, D. Effect of Hydrogen Trapping on Void Growth and Coalescence in Metals and Alloys. *Mech. Mater.* **2008**, *40*, 115–132. [[CrossRef](#)]
174. Wang, Y.; Sharma, B.; Xu, Y.; Shimizu, K.; Fujihara, H.; Hirayama, K.; Takeuchi, A.; Uesugi, M.; Cheng, G.; Toda, H. Switching Nanoprecipitates to Resist Hydrogen Embrittlement in High-Strength Aluminum Alloys. *Nat. Commun.* **2022**, *13*, 6860. [[CrossRef](#)] [[PubMed](#)]
175. Nielsen, C.; Amirkhizi, A.V.; Nemat-Nasser, S. An Empirical Model for Estimating Fracture Toughness Using the DCDC Geometry. *Int. J. Fract.* **2014**, *188*, 113–118. [[CrossRef](#)]
176. Begum, Y.; Bharath, K.N.; Doddamani, S.; Rajesh, A.M.; Kaleemulla, K.M. Optimization of Process Parameters of Fracture Toughness Using Simulation Technique Considering Aluminum–Graphite Composites. *Trans. Indian Inst. Met.* **2020**, *73*, 3095–3103. [[CrossRef](#)]
177. Abdellah, M.Y.; Hassan, M.K.; Hashem, A.M. Finite Element Computational Approach of Fracture Toughness in Composite Compact-Tension Specimen. *Int. J. Mech. Mechatron. Eng.* **2012**, *12*, 57–61.
178. Achebo, J. Development of a Predictive Model for Determining Mechanical Properties of AA 6061 Using Regression Analysis. *Prod. Manuf. Res.* **2015**, *3*, 169–184. [[CrossRef](#)]
179. Gander, M.J.; Hennicker, J.; Masson, R. Modeling and Analysis of the Coupling in Discrete Fracture Matrix Models. *SIAM J. Numer. Anal.* **2021**, *59*, 195–218. [[CrossRef](#)]
180. Zhong, Y.; Shao, Y.; Gao, X.; Luo, X.; Zhu, H. Fatigue Crack Growth of EH36 Steel in Air and Corrosive Marine Environments. *J. Constr. Steel Res.* **2023**, *210*, 108104. [[CrossRef](#)]
181. Vishnuvardhan, S.; Saravanan, M.; Gandhi, P.; Raghava, G. Fatigue Crack Growth Studies on Power Plant Piping Materials under Corrosive Environment. *Procedia Struct. Integr.* **2019**, *14*, 482–490. [[CrossRef](#)]
182. Brückner, A.; Munz, D. The Effect of Curve Fitting on the Prediction of Failure Probabilities from the Scatter in Crack Geometry and Fracture Toughness. *Reliab. Eng.* **1983**, *5*, 139–156. [[CrossRef](#)]
183. Guddhur, H.; Naganna, C.; Doddamani, S. Taguchi’s Method of Optimization of Fracture Toughness Parameters of Al-SiCp Composite Using Compact Tension Specimens. *Int. J. Optim. Control. Theor. Appl.* **2021**, *11*, 152–157. [[CrossRef](#)]
184. Younis, H.B.; Kamal, K.; Sheikh, M.F.; Hamza, A. Prediction of Fatigue Crack Growth Rate in Aircraft Aluminum Alloys Using Optimized Neural Networks. *Theor. Appl. Fract. Mech.* **2022**, *117*, 103196. [[CrossRef](#)]
185. Kovalov, D.; Fekete, B.; Engelhardt, G.R.; Macdonald, D.D. Prediction of Corrosion Fatigue Crack Growth Rate in Alloys. Part II: Effect of Electrochemical Potential, NaCl Concentration, and Temperature on Crack Propagation in AA2024-T351. *Corros. Sci.* **2019**, *152*, 130–139. [[CrossRef](#)]
186. Zhang, T.; He, Y.; Li, C.; Zhang, T.; Zhang, S. Effect of Alternate Corrosion and Fatigue on Fatigue Crack Growth Characterization of 2024-T4 Aluminum Alloy. *Math. Probl. Eng.* **2020**, *2020*, 7314241. [[CrossRef](#)]
187. Bergner, F.; Zouhar, G. New Approach to the Correlation between the Coefficient and the Exponent in the Power Law Equation of Fatigue Crack Growth. *Int. J. Fatigue* **2000**, *22*, 229–239. [[CrossRef](#)]
188. Alqahtani, I.; Starr, A.; Khan, M. Investigation of the Combined Influence of Temperature and Humidity on Fatigue Crack Growth Rate in Al6082 Al-Loy in a Coastal Environment. *Materials* **2023**, *16*, 6833. [[CrossRef](#)]
189. He, F.; Khan, M.; Aldosari, S. Interdependencies between Dynamic Response and Crack Growth in a 3D-Printed Acrylonitrile Butadiene Styrene (ABS) Cantilever Beam under Thermo-Mechanical Loads. *Polymers* **2022**, *14*, 982. [[CrossRef](#)] [[PubMed](#)]
190. Yang, Y.; Chen, H.; Feng, W.; Xu, S.; Li, Y.; Zhang, R. Fatigue Life Analysis for 6061-T6 Aluminum Alloy Based on Surface Roughness. *PLoS ONE* **2021**, *16*, e0252772. [[CrossRef](#)] [[PubMed](#)]
191. Zai, B.A.; Khan, M.; Khan, S.Z.; Asif, M.; Khan, K.A.; Saquib, A.N.; Mansoor, A.; Shahzad, M.; Mujtaba, A. Prediction of Crack Depth and Fatigue Life of an Acrylonitrile Butadiene Styrene Cantilever Beam Using Dynamic Response. *J. Test. Eval.* **2020**, *48*, 1520–1536. [[CrossRef](#)]
192. Guo, M.; Li, D.; Rao, S.X.; Guo, B.L. Effect of Environmental Factors on the Corrosion of 2024T3 Aluminium Alloy. In Proceedings of the 9th International Conference on Aluminium Alloys, Brisbane, Australia, 2–5 August 2004; Nie, J.F., Morton, A.J., Muddle, B.C., Eds.; Institute of Materials Engineering Australasia Ltd.: Melbourne, Australia, 2004; pp. 433–438.
193. Ichitani, K. Effect of Experimental Humidity on Fatigue Fracture of 6XXX-Series Aluminum Alloys. *Mater. Sci. Eng.* **2012**, 15–21.
194. Bayoumi, M. Fatigue Behaviour of a Commercial Aluminium Alloy in Sea Water at Different Temperatures. *Eng. Fract. Mech.* **1993**, *45*, 297–307. [[CrossRef](#)]
195. Khan, M.A.; Khan, S.Z.; Sohail, W.; Khan, H.S.M.; Nisar, S. Mechanical Fatigue in Aluminum at Elevated Temperature and Remaining Life Prediction Based on Natural Frequency Evolution. *Fatigue Fract. Eng. Mater. Struct.* **2015**, *38*, 897–903. [[CrossRef](#)]
196. Omar, I.K.M.; Starr, A. Comparative Analysis of Machine Learning Models for Predicting Crack Propagation under Coupled Load and Temperature. *Appl. Sci.* **2023**, *13*, 7212. [[CrossRef](#)]
197. He, F.; Khan, M. Effects of Printing Parameters on the Fatigue Behaviour of 3d-Printed Abs under Dynamic Thermo-Mechanical Loads. *Polymers* **2021**, *13*, 2362. [[CrossRef](#)]
198. Kamei, K.; Khan, M.A. Current Challenges in Modelling Vibrational Fatigue and Fracture of Structures: A Review. *J. Braz. Soc. Mech. Sci. Eng.* **2020**, *43*, 77. [[CrossRef](#)]

199. Agala, A.; Khan, M.; Starr, A. Degradation Mechanisms Associated with Metal Pipes and the Effective Impact of LDMs and LLMs in Water Transport and Distribution. *Proc. Inst. Mech. Eng. Part C J. Mech. Eng. Sci.* **2023**, *237*, 1855–1876. [[CrossRef](#)]
200. Khan, S.Z.; Khan, T.M.; Joya, Y.F.; Khan, M.A.; Ahmed, S.; Shah, A. Assessment of Material Properties of AISI 316L Stainless Steel Using Non-Destructive Testing. *Nondestruct. Test. Eval.* **2016**, *31*, 360–370. [[CrossRef](#)]
201. Gairola, S.; Rengaswamy, J.; Verma, R. A Study on XFEM Simulation of Tensile, Fracture Toughness, and Fatigue Crack Growth Behavior of Al 2024 Alloy through Fatigue Crack Growth Rate Models Using Genetic Algorithm. *Fatigue Fract. Eng. Mater. Struct.* **2023**, *46*, 2121–2138. [[CrossRef](#)]
202. Hareesha, G.; Chikkanna, N.; Doddamani, S. Finite Element Simulation of Fracture Toughness of Al6061 Reinforced with Silicon Carbide. *IOP Conf. Ser. Mater. Sci. Eng.* **2021**, *1065*, 012036. [[CrossRef](#)]
203. Saleemsab Doddamani, M.K. Indentation Fracture Toughness of Aluminum6061-Graphite Composites. *Int. J. Fract. Damage Mech.* **2016**, *1*, 40–46.
204. Zhou, Z.; Bhamare, S.; Qian, D. Ductile Fracture in Thin Sheet Metals: A FEM Study of the Sandia Fracture Challenge Problem Based on the Gurson–Tvergaard–Needleman Fracture Model. *Int. J. Fract.* **2014**, *186*, 185–200. [[CrossRef](#)]
205. Chen, Z.; Dai, Y.; Liu, Y. Life Prediction of Corrosion-Fatigue Based on a New Crack Growth Rate Model with Damage and the Extended Finite Element Method. *Eng. Fract. Mech.* **2023**, *289*, 109445. [[CrossRef](#)]
206. Huang, Y.; Ye, X.; Hu, B.; Chen, L. Equivalent Crack Size Model for Pre-Corrosion Fatigue Life Prediction of Aluminum Alloy 7075-T6. *Int. J. Fatigue* **2016**, *88*, 217–226. [[CrossRef](#)]
207. Hu, P.; Meng, Q.; Hu, W.; Shen, F.; Zhan, Z.; Sun, L. A Continuum Damage Mechanics Approach Coupled with an Improved Pit Evolution Model for the Corrosion Fatigue of Aluminum Alloy. *Corros. Sci.* **2016**, *113*, 78–90. [[CrossRef](#)]
208. Safyari, M.; Khossossi, N.; Meisel, T.; Dey, P.; Prohaska, T.; Moshtaghi, M. New Insights into Hydrogen Trapping and Embrittlement in High Strength Aluminum Alloys. *Corros. Sci.* **2023**, *223*, 111453. [[CrossRef](#)]
209. Gholami, M.D.; Hashemi, R.; Sedighi, M. The Effect of Temperature on the Mechanical Properties and Forming Limit Diagram of Aluminum Strips Fabricated by Accumulative Roll Bonding Process. *J. Mater. Res. Technol.* **2020**, *9*, 1831–1846. [[CrossRef](#)]
210. Mouritz, A.P. 19—Fracture Toughness Properties of Aerospace Materials. In *Introduction to Aerospace Materials*; Mouritz, A.P., Ed.; Woodhead Publishing: Sawston, UK, 2012; pp. 454–468. ISBN 9781855739468.

**Disclaimer/Publisher’s Note:** The statements, opinions and data contained in all publications are solely those of the individual author(s) and contributor(s) and not of MDPI and/or the editor(s). MDPI and/or the editor(s) disclaim responsibility for any injury to people or property resulting from any ideas, methods, instructions or products referred to in the content.